Geologic history of Siletzia, a large igneous province in the Oregon and Washington Coast Range: Correlation to the geomagnetic polarity time scale and implications for a long-lived Yellowstone hotspot

Geologic history of Siletzia, a large igneous province in the Oregon and Washington Coast Range: Correlation to the geomagnetic polarity time scale and implications for a long-lived Yellowstone hotspot

Ray Wells[1], David Bukry[1], Richard Friedman[2], Doug Pyle[3], Robert Duncan[4], Peter Haeussler[5], and Joe Wooden[6]

[1]*U.S. Geological Survey, 345 Middlefield Road, Menlo Park, California 94025-3561, USA*
[2]*Pacific Centre for Isotopic and Geochemical Research, Department of Earth, Ocean and Atmospheric Sciences, 6339 Stores Road, University of British Columbia, Vancouver, BC V6T 1Z4, Canada*
[3]*Department of Geology and Geophysics, University of Hawaii at Manoa, 1680 East West Road, Honolulu, Hawaii 96822, USA*
[4]*College of Earth, Ocean, and Atmospheric Sciences, Oregon State University, 104 CEOAS Administration Building, Corvallis, Oregon 97331-5503, USA*
[5]*U.S. Geological Survey, 4210 University Drive, Anchorage, Alaska 99508-4626, USA*
[6]*School of Earth Sciences, Stanford University, 397 Panama Mall Mitchell Building 101, Stanford, California 94305-2210, USA*

ABSTRACT

Siletzia is a basaltic Paleocene and Eocene large igneous province in coastal Oregon, Washington, and southern Vancouver Island that was accreted to North America in the early Eocene. New U-Pb magmatic, detrital zircon, and $^{40}Ar/^{39}Ar$ ages constrained by detailed field mapping, global nannoplankton zones, and magnetic polarities allow correlation of the volcanics with the 2012 geologic time scale. The data show that Siletzia was rapidly erupted 56–49 Ma, during the Chron 25–22 plate reorganization in the northeast Pacific basin. Accretion was completed between 51 and 49 Ma in Oregon, based on CP11 (CP—Coccolith Paleogene zone) coccoliths in strata overlying onlapping continental sediments. Magmatism continued in the northern Oregon Coast Range until ca. 46 Ma with the emplacement of a regional sill complex during or shortly after accretion. Isotopic signatures similar to early Columbia River basalts, the great crustal thickness of Siletzia in Oregon, rapid eruption, and timing of accretion are consistent with offshore formation as an oceanic plateau. Approximately 8 m.y. after accretion, margin parallel extension of the forearc, emplacement of regional dike swarms, and renewed magmatism of the Tillamook episode peaked at 41.6 Ma (CP zone 14a; Chron 19r). We examine the origin of Siletzia and consider the possible role of a long-lived Yellowstone hotspot using the reconstruction in GPlates, an open source plate model. In most hotspot reference frames, the Yellowstone hotspot (YHS) is on or near an inferred northeast-striking Kula-Farallon and/or Resurrection-Farallon ridge between 60 and 50 Ma. In this configuration, the YHS could have provided a 56–49 Ma source on the Farallon plate for Siletzia, which accreted to North America by 50 Ma. A sister plateau, the Eocene basalt basement of the Yakutat terrane, now in Alaska, formed contemporaneously on the adjacent Kula (or Resurrection) plate and accreted to coastal British Columbia at about the same time. Following accretion of Siletzia, the leading edge of North America overrode the YHS ca. 42 Ma. The voluminous high-Ti basaltic to alkalic magmatism of the 42–35 Ma Tillamook episode and extension in the forearc may be related to the encounter with an active YHS. Clockwise rotation of western Oregon about a pole in the backarc has since moved the Tillamook center and underlying Siletzia northward ~250 km from the probable hotspot track on North America. In the reference frames we examined, the YHS arrives in the backarc ~5 m.y. too early to match the 17 Ma magmatic flare-up commonly attributed to the YHS. We suggest that interaction with the subducting slab may have delayed arrival of the plume beneath the backarc.

INTRODUCTION

Basement rocks of the Oregon and Washington Coast Ranges (northwest USA) consist of thick basaltic sequences of Paleocene and Eocene age that are exposed in anticlinal uplifts from southern Vancouver Island (Canada) to Roseburg, Oregon (Fig. 1). These volcanic complexes include the Siletz River Volcanics (SRV) of Oregon, the Crescent Formation of Washington, and the Metchosin igneous complex of southern Vancouver Island. They are composed dominantly of tholeiitic and alkalic submarine and subaerial basalt, with attendant intrusive rocks, submarine breccias, marine sediments, and rare silicic flows that formed islands and seamounts built on ocean crust (Snavely et al., 1968). Together, they compose a large oceanic terrane that was accreted to North America in the Eocene (Snavely and MacLeod, 1974; Simpson and Cox, 1977; Duncan, 1982; Heller and Ryberg, 1983; Wells et al., 1984; McCrory and Wilson, 2013). The SRV and onlapping strata of the Oregon Coast Range have undergone large, clockwise paleomagnetic rotation (e.g., Simpson and Cox, 1977). The SRV is thought to be an allochthonous terrane, although latitudinal transport is small, probably no more than a few hundred kilometers (Beck, 1984). We consider all of these units part of Siletzia, after Irving (1979). Siletzia is thus a composite terrane, composed of the Crescent terrane of Washington and British Columbia and the Siletz terrane of Oregon, which are similar in composition, age, and history, but have undergone variable amounts of tectonic rotation (e.g., McCrory and Wilson, 2013).

Beneath western Oregon, in the present forearc, Trehu et al. (1994) documented high-velocity mafic crust 22–32 km thick; they suggested that it represented an accreted oceanic plateau (Fig. 2). The eastern extent of the oceanic crust beneath the volcanic cover of the Columbia

Geosphere; August 2014; v. 10; no. 4; p. 692–719; doi:10.1130/GES01018.1; 16 figures; 1 supplemental file.
Received 24 December 2013 ♦ Revision received 7 May 2014 ♦ Accepted 25 June 2014 ♦ Published online 14 July 2014

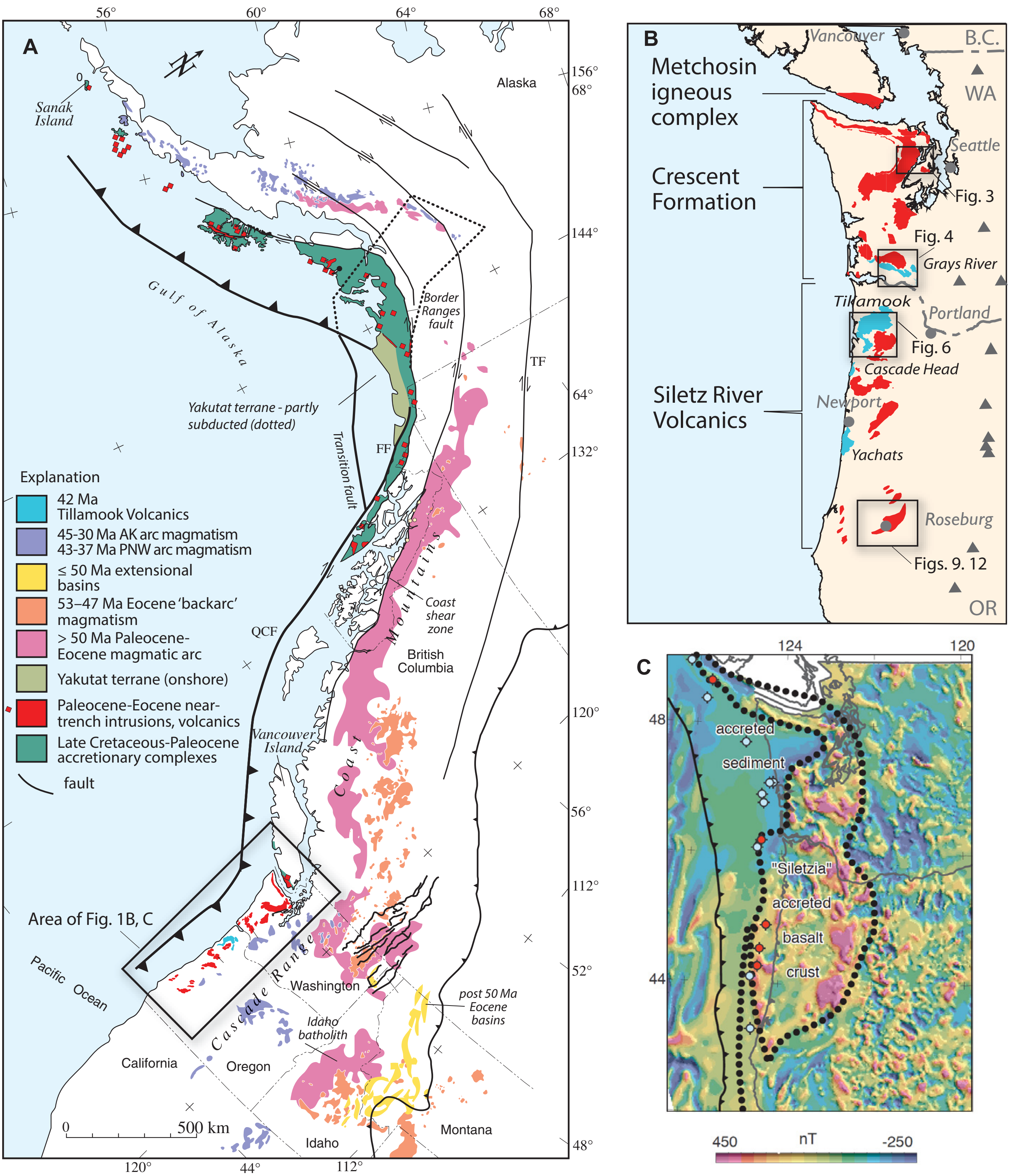

Figure 1. Tectonic setting of Siletzia. (A) Regional setting showing Paleocene–Eocene continental margin magmatism and location of oceanic Siletzia and Yakutat terranes (from Haeussler et al., 2003). FF—Fairweather Fault; QCF—Queen Charlotte Fault; TF—Tintina fault. (B) Formations composing Siletzia (red) and postaccretion basaltic magmatism (blue, from McCrory and Wilson, 2013). OR—Oregon; WA—Washington; B.C.—British Columbia. (C) Extent of Siletzia in the subsurface from regional aeromagnetic data and deep exploration wells (red bottoms in basalt, blue in sediments; from Wells et al., 1998).

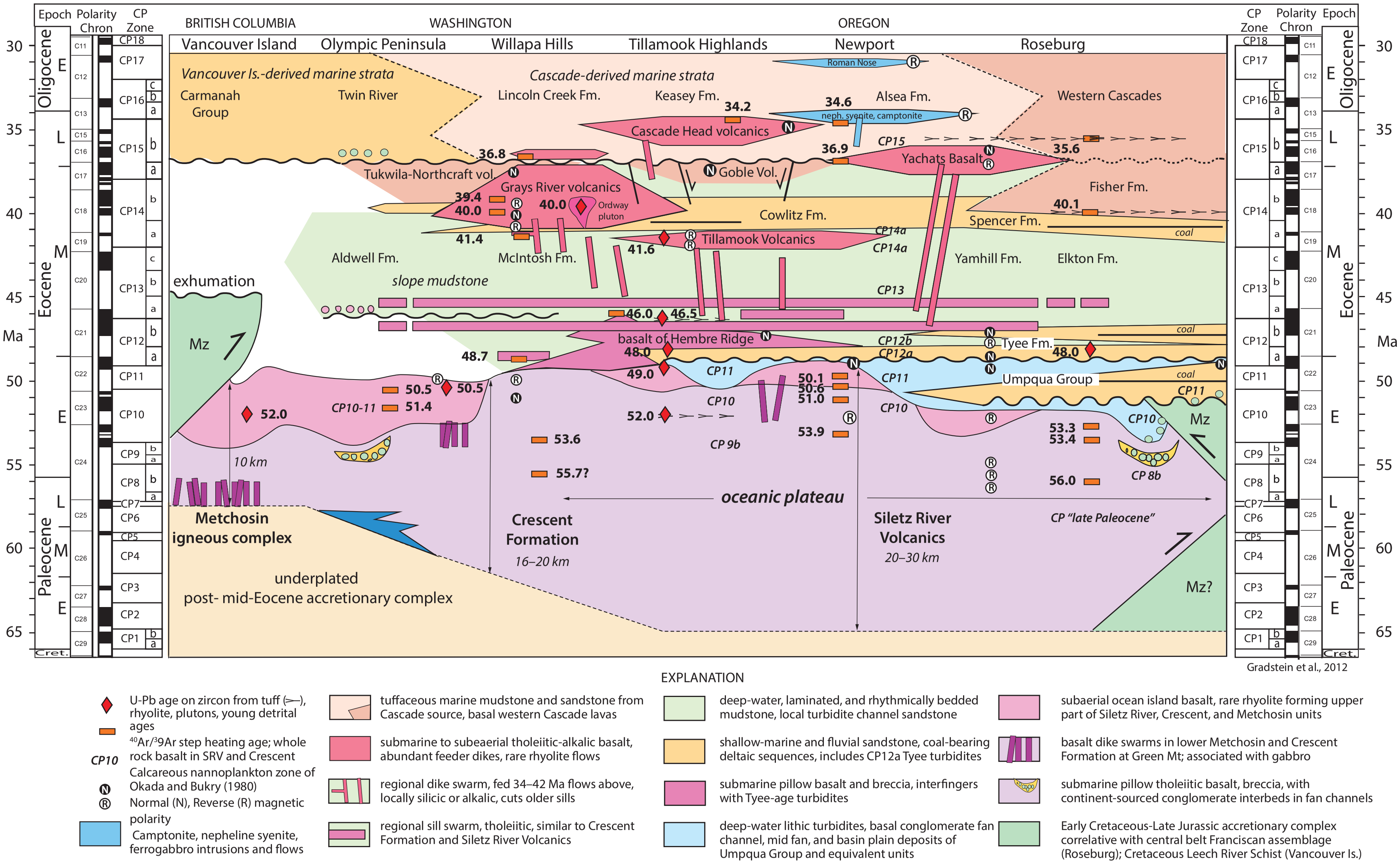

Figure 2. Siletzia time-rock diagram roughly parallel to subduction margin; time scale of Gradstein et al. (2012). Data sources: Vancouver Island geology: Yorath et al. (1999); Massey (1986); Groome et al. (2003). Vancouver Island isotopic ages: Yorath et al. (1999), Groome et al. (2003). Olympic Peninsula geology: Tabor and Cady (1978); Babcock et al. (1992); Snavely et al. (1993b); Haeussler and Clark (2000); Hirsch and Babcock (2009); Tabor et al. (2011). Olympic Peninsula isotopic ages: Haeussler and Clark (2000); Babcock and Hirsch (2006). Olympic Peninsula CP zones: Bukry, *in* Snavely et al. (1993b); Squires et al. (1992). Willapa Hills geology: Wolfe and McKee (1968); Wells (1981, 1989a); Moothart (1993); Kleibacker (2001); Payne (1998). Willapa Hills isotopic ages: Chan et al. (2012). Willapa Hills magnetic polarity: Wells and Coe (1985). Tillamook Highlands geology: Wells et al. (1995); Niem and Niem (1985); Snavely et al. (1996). Tillamook Highlands isotopic ages: this paper. Tillamook Highlands CP zones: Bukry and Snavely (1988); Bukry, *in* Wells et al. (1995); this paper. Tillamook Highlands magnetic polarity: Magill et al. (1981); Beck and Plumley (1980). Newport geology: Snavely et al. (1976a, 1976b, 1976c); Walker and Duncan (1988). Newport isotopic ages: Pyle et al. (2009). Newport CP zones: Bukry and Snavely (1988). Newport magnetic polarity: Simpson (1977); Beck and Plumley (1980). Roseburg geology: Wells et al. (2000). Roseburg isotopic ages: Pyle et al. (2009). Roseburg CP zones: Bukry and Snavely (1988); Bukry *in* Wells et al. (2000); this paper. Roseburg magnetic polarity: Simpson (1977); Wells et al. (2000). E, M, L are informal early, middle, and late subdivisions of Cenozoic epochs; Cret. represents the Cretaceous Period.

Embayment is the subject of some debate. Early workers considered that the entire embayment might be floored with early Cenozoic oceanic basalt (e.g., Hamilton and Myers, 1966). Based on its variable seismic thickness and aeromagnetic extent (Fig. 1), the unsubducted portion of the Siletz and Crescent terranes comprises 1.7–2.6 × 10^6 km^3, 8–12 times the erupted volume of the Columbia River flood basalt province (Reidel, 2013). Siletzia is a large igneous province in the classification of Bryan and Ernst (2008). The large volume of basalt may indicate an origin at a hotspot, and the mantle source for the basalts has Pb and Nd isotopic similarities to the source that melted to produce the early Columbia River flood basalts (Pyle et al., 2009). Previously it was argued that a long-lived Yellowstone hotspot (YHS) was responsible for the creation of Siletzia (e.g., Duncan, 1982; Murphy et al., 2003), and the implications of this event for Cordilleran evolution are substantial.

Others considered the coastal basalts to be the product of marginal rifting of North America during ridge subduction (Wells et al., 1984; Massey, 1986; Clowes et al., 1987; Snavely, 1987), producing slab window volcanism (Babcock et al., 1992; Thorkelson, 1996; Groome et al., 2003; Haeussler et al., 2003; Breitsprecher et al., 2003). Sheeted dikes in the Metchosin igneous complex of Vancouver Island and locally in the Crescent Formation, along with their transitional chemistry (Massey, 1986), are consistent with marginal rifting, as is the tholeiitic and alkalic volcanism in the Coast Range that continued for 20 m.y. after suturing of Siletzia to the margin. In Wells et al. (1984) it was hypothesized that part of the marginal rift basin and outboard terranes were transported northward by plate motion and accreted to southern Alaska. The Yakutat terrane of southern Alaska has basalt basement compositions, stratigraphy, and a structural history similar to Siletzia (Plafker, 1987; Davis and Plafker, 1986), and may be related (Fig. 1). Christeson et al. (2010) and Worthington et al. (2012) documented that the crustal velocity structure of the Yakutat terrane is similar to a mafic oceanic plateau.

In Haeussler et al. (2003) it was suggested that the Eocene sweep of near-trench magmatism across northeast Pacific marginal terranes from Alaska to Oregon was the result of the subduction of an additional plate, the Resurrection plate, and its bounding ridges. McCrory and Wilson (2013) proposed that Siletzia consists of two terranes, the Siletz and Crescent, which were accreted, along with the Yakutat terrane, during breakup and rotation of fragments of the Resurrection and Farallon plates.

Schmandt and Humphreys (2011) and Gao et al. (2011) revisited the docking of Siletzia. The mantle tomography of both Schmandt and Humphreys (2011) and Gao et al. (2011) shows a high-velocity curtain hanging in the asthenosphere beneath Idaho, and they suggested that an attached, remnant Farallon slab is underplated beneath the Pacific Northwest; they view the docking of Siletzia as the cause of a tear between Siletzia and the still-subducting, flat Farallon slab to the south, with rollback of the slab from the tear causing the mid-Cenozoic southward migration of magmatism in the Cordillera.

This view of a large accreted Siletz terrane attached to a stalled Farallon slab beneath the Pacific Northwest appears incompatible with the marginal rift and slab window models for Siletzia. Here we provide new age constraints and field observations on the origin of Siletzia, the timing of its attachment to North America, and the timing of postaccretion magmatism to partly resolve this conundrum. We also investigate the structural relation of Siletzia to the Yakutat terrane and to the development of the Columbia Embayment.

APPROACH

Our analysis is based on our geologic mapping of Siletzia over the past three decades (Wells, 1981, 1989a; Wells et al., 1995, 2000; Wells and Sawlan, 2014), building on the earlier framework by Snavely et al. (1976a, 1976b, 1976c, 1993b, 1996) and Tabor and Cady (1978). Age assignments of marine strata interfingering and overlying the basalts of Siletzia are based on the calcareous nannoplankton (coccolith) framework, which is tied to the global biostratigraphic zonation (Bukry, 1971, 1973; CP—Coccolith Paleogene zones of Okada and Bukry, 1980; Bukry and Snavely, 1988, Gradstein et al., 2012). Coccolith samples have been systematically collected from Coast Range strata for more than four decades; selected samples relevant to this study are listed in Table DR1 in the Supplemental File[1]. Paleomagnetic sampling with portable drilling equipment was also done during mapping to better understand the timing of tectonic rotation and its relation to suturing of Siletzia to the margin. The paleomagnetic studies (Wells and Coe, 1985; Wells et al., 2000), along with the work of Simpson and Cox (1977) and Magill et al. (1981), also provide a magnetic polarity stratigraphy useful for correlation with the time scale.

Rare rhyolite flows, silicic tuff interbeds, and sedimentary interbeds in the dominantly basaltic terrane provided targets for direct U-Pb dating of volcanic events and studies of detrital zircon populations in the sedimentary interbeds. We collected nine samples from tuff interbeds in the SRV and overlying sedimentary sequence, and from rhyolite in the Tillamook Volcanics; four contained zircons suitable for analysis on the thermal ionization mass spectrometer at the University of British Columbia (Tables DR2 and DR3 in the Supplemental File [see footnote 1]; see Appendix 1 for analytical details). We also collected zircons from an ash flow tuff near the top of the SRV and from a pluton in the Grays River volcanics that were analyzed on the sensitive high-resolution ion microprobe at the Australian National University (Table DR4 in the Supplemental File [see footnote 1]). We analyzed two detrital zircon populations from the Tyee Formation (collected by J. Vance, University of Washington), and one collected in the Wilson River, Oregon (by us), reported in Dumitru et al. (2013). We also analyzed a zircon suite from the Blue Mountain sedimentary unit, which interfingers with the base of the Crescent Formation basalt at Buckhorn Mountain on the Olympic Peninsula (Table DR5 in the Supplemental File [see footnote 1]; collected by J. Vance).

We compare our U-Pb and coccolith ages to $^{40}Ar/^{39}Ar$ ages for the SRV and overlying volcanic rocks (Pyle et al., 2009), summarized in Table DR6 in the Supplemental File (see footnote 1). The isotopic ages, calcareous nannoplankton ages, and magnetic polarity data are used to tie Siletzia's history to the geomagnetic polarity time scale (GPTS; Gradstein et al., 2012). We then use GPlates 1.3, an open source global plate motion model (Boyden et al., 2011; Gurnis et al., 2012; Seton et al., 2012) to examine the origin and accretion of Siletzia, the extent of other Siletz-like terranes in the northeast Pacific, and the possible role of a hotspot in producing the large volumes of basalt. We make no assumptions about the origin of the hotspot, except to note that well-documented hotspot magma sources can last for tens of millions of years, produce large volumes of magma, and move more slowly than overlying plates (e.g., Courtillot et al., 2003).

[1]Supplemental File. Zipped file containing: (1) 6 tables: Table DR1: Coccolith CP zones in Oregon and Washington Coast Range Paleogene strata; Table DR2: U-Pb TIMS ages, Tillamook Highlands, OR; Table DR3: U-Pb TIMS data, Tillamook Highlands, OR; Table DR4: U-Pb SHRIMP ages, Siletz R. Volcanics and Grays R. Volcanics, OR and WA; Table DR5: Detrital Zircon ages, Tyee Fm. OR and base of Crescent Fm. WA; Table DR6: $^{40}Ar/^{39}Ar$ plateau ages for OR-WA Siletz River Volcanics; (2) a Word doc describing the animation of origin and accretion of Siletzia and Yakutat terranes in GPlates; and (3) a .mov file containing Siletzia-Yakutat terrane origin and accretion.mov. If you are viewing the PDF of this paper or reading it offline, please visit http://dx.doi.org/10.1130/GES01018.S1 or the full-text article on www.gsapubs.org to view the Supplemental File.

STRATIGRAPHIC FRAMEWORK OF THE CRESCENT, SILETZ, AND YAKUTAT TERRANES

Although deformed by folding and thrusting during accretion, Siletzia is a relatively coherent terrane with mappable stratigraphy (Fig. 2; see references in Fig. 2 caption). It consists mostly of late Paleocene to early Eocene deep-marine tholeiitic pillow basalt interbedded with thin, bathyal sedimentary interbeds and locally overlain by subaerial flows. The base of Siletzia is not exposed, except in the Olympic Mountains, where 16.5 km of Crescent Formation basalt is tilted to vertical by doming of the Olympic Mountains sedimentary accretionary complex thrust beneath it (Tabor and Cady, 1978; Hirsch and Babcock, 2009). Active source seismic experiments show that the basaltic crust of the forearc thickens southward from 10 km beneath Vancouver Island to 20 km beneath Washington and as much as 30 km beneath Oregon (Clowes et al., 1987; Trehu et al., 1994; Parsons et al., 1998, 1999). We discuss the Siletz and the Crescent terranes separately because the great variation in crustal thickness may suggest different histories (i.e., McCrory and Wilson, 2013). Descriptions that follow are derived from the original mapping and are summarized in Figure 2. Ages of nannoplankton (CP—Coccolith Paleogene zones; defined by Bukry, 1971, 1973; Okada and Bukry, 1980) are keyed to the time scale of Gradstein et al. (2012).

Crescent Terrane

Vancouver Island

We include in the Crescent terrane exposures of Eocene basalt and gabbro of the Metchosin igneous complex that crop out on southern Vancouver Island (Yorath et al., 1999; Fig. 1) and appear to be continuous with exposures on the Olympic Peninsula, based on seismic, well, and potential field data. The Metchosin igneous complex consists of blocky basalt and pillow basalt overlying gabbro and a sheeted dike swarm, all thrust beneath the Cretaceous Leech River schist along the Leech River fault (Groome et al., 2003). Yorath et al. (1999) reported U-Pb ages of 52 and 54 Ma from the volcanics, which are lower greenschist grade. Yorath et al. (1999) considered the chemistry to be transitional between oceanic and arc affinity and suggested that the basalts were produced during marginal rifting. This interpretation is consistent with the relatively thin crust, sheeted dike swarms, and the nearby bimodal 50 Ma Flores volcanics erupted through pre-Cenozoic terranes along the coast (Madsen et al., 2006). Seismic profiling shows the Metchosin complex to be ~10 km thick and underthrust beneath Vancouver Island (Clowes et al., 1987). Underthrusting of the Metchosin basalts at 45 Ma is inferred from $^{40}Ar/^{39}Ar$ cooling ages of mica in the uplifted Leech River schist and onlap of the Carmanah Group sediments ca. 35 Ma (Groome et al., 2003).

Olympic Mountains and Adjacent Areas

Thick submarine and subaerial basalt flows of the Crescent Formation form a horseshoe-shaped outcrop in fault contact with the sedimentary accretionary complex forming the core of the Olympic Mountains in Washington (Fig. 1). The deep-water basal pillow basalt overlies and interfingers with lithic turbidite sandstone and mudstone of the Blue Mountain unit, and both are underthrust by the younger accretionary complex, which contains slivers of basalt similar to the Crescent Formation (Tabor and Cady, 1978). As much as 16.5 km of basalt is exposed in the eastern Olympic Mountains, where the lower part is lower greenschist facies metamorphic grade, presumably due to burial (Hirsch and Babcock, 2009; Blakely et al., 2009). North of the Big Quilcine River, the pillow basalt contains a debris flow deposit with rounded boulders of hornblende quartz diorite as much as 3 m in diameter, with a K-Ar age of 53.4 Ma on hornblende (Tabor and Cady, 1978). The upper part of the Crescent Formation is blocky to columnar jointed basalt with oxidized flow contacts indicative of subaerial eruption and more typical zeolite and smectitic clay alteration, as seen elsewhere in the Coast Range. The Crescent Formation exposures on the Olympic Peninsula span an area a bit larger than the island of Hawaii, and the 16.5 km thickness of the formation is about the same as the 17 km thickness of Mauna Loa, if subsidence of the seafloor is accounted for (Lipman, 1995; Lipman and Calvert, 2013). Seismic profiling indicates that the Crescent Formation is continuous, with high-velocity crust that extends northward to the Metchosin complex, east beneath Puget Sound, and south to the Willapa Hills and Oregon (Trehu et al., 1994; Parsons et al., 1999; Brocher et al., 2001). Chemically, the basalt is typical of oceanic island and ocean floor composition; Babcock et al. (1992) proposed that it formed in a slab window environment during ridge subduction. Rare silicic flows occur near the top of the formation at Striped Peak (Tabor and Cady, 1978; Snavely et al., 1993b).

Whole-rock $^{40}Ar/^{39}Ar$ ages of basalt range from 51.0 ± 4.7 Ma at the base of the subaerial section to 50.5 ± 1.6 Ma at the top (Babcock and Hirsch, 2006), consistent with a 50.5 Ma U-Pb zircon age from nearby Green Mountain (Haeussler and Clark, 2000; Tabor et al., 2011) and calcareous nannoplankton zones CP10 and 11 (53.5–49 Ma; all CP zone ages are from time scale of Gradstein et al., 2012) from mudstone interbeds in basalt flows near the top of the Crescent Formation at Pulali Point (Squires et al., 1992). Detrital zircons from the Blue Mountain unit sediments that interfinger with the base of Crescent pillow basalt at Buckhorn Mountain (Fig. 3; JV 440, Table DR5 in the Supplemental File [see footnote 1]) are primarily Cretaceous, but 4 grains have a young peak ca. 49 Ma, within the uncertainties of the $^{40}Ar/^{39}Ar$ ages near the top of the section. Buckhorn Mountain is ~9 km north of the 16.5-km-thick measured section of Hirsch and Babcock (2009). If future work can confirm the young basal age, the entire Crescent section may have accumulated in <1 m.y., a rate similar to the construction of Mauna Loa (Lipman, 1995; Lipman and Calvert, 2013).

Willapa Hills

The Crescent Formation in the Willapa Hills (Figs. 1 and 4) is exposed in broad, faulted anticlinoria and consists of aphyric pillow basalt and columnar jointed basalt, basalt breccia, diabase, and gabbro (Wells, 1981; Wells and Sawlan, 2014). The pillow basalt forms large sheet flows and feeder tubes (Fig. 5), similar to the upper part of the SRV in Oregon (Snavely et al., 1968). Locally the pillow basalt is overlain by porphyritic, subaerial columnar and blocky jointed basalt flows, vesicular submarine basalt lapilli breccias, and fringing fossiliferous shallow-water basaltic sandstones characteristic of an oceanic island environment (Wells, 1981; Wells and Sawlan, 2014). The basalt composition is tholeiitic to alkalic (Moothart, 1993).

Step-heating $^{40}Ar/^{39}Ar$ ages of 55.7 ± 1.0 Ma and 53.6 ± 2.0 Ma were reported from the pillow basalt (Moothart, 1993), although the ages may be affected by inheritance. Magnetically reversed flows overlie normal flows in the Crescent Formation of the Willapa Hills (Wells and Coe, 1985). No calcareous nannoplankton have been recovered from the Crescent Formation in the Willapa Hills. Deformation of the anticlinoria and local block rotation occurred during or following accretion and before onlap of late-middle Eocene coal-bearing sandstone of the Cowlitz Formation (Wells and Coe, 1985). The dominant columnar jointed unit, which composes ~50% of the outcrop, is part of a regional basalt, diabase, and gabbro sill swarm that was emplaced along thin sedimentary interbeds into the upper Crescent Formation and into the overlying Eocene deep-water mudstones. This late magmatic event occurred near the time of accretion of the Crescent terrane and is discussed in more detail herein.

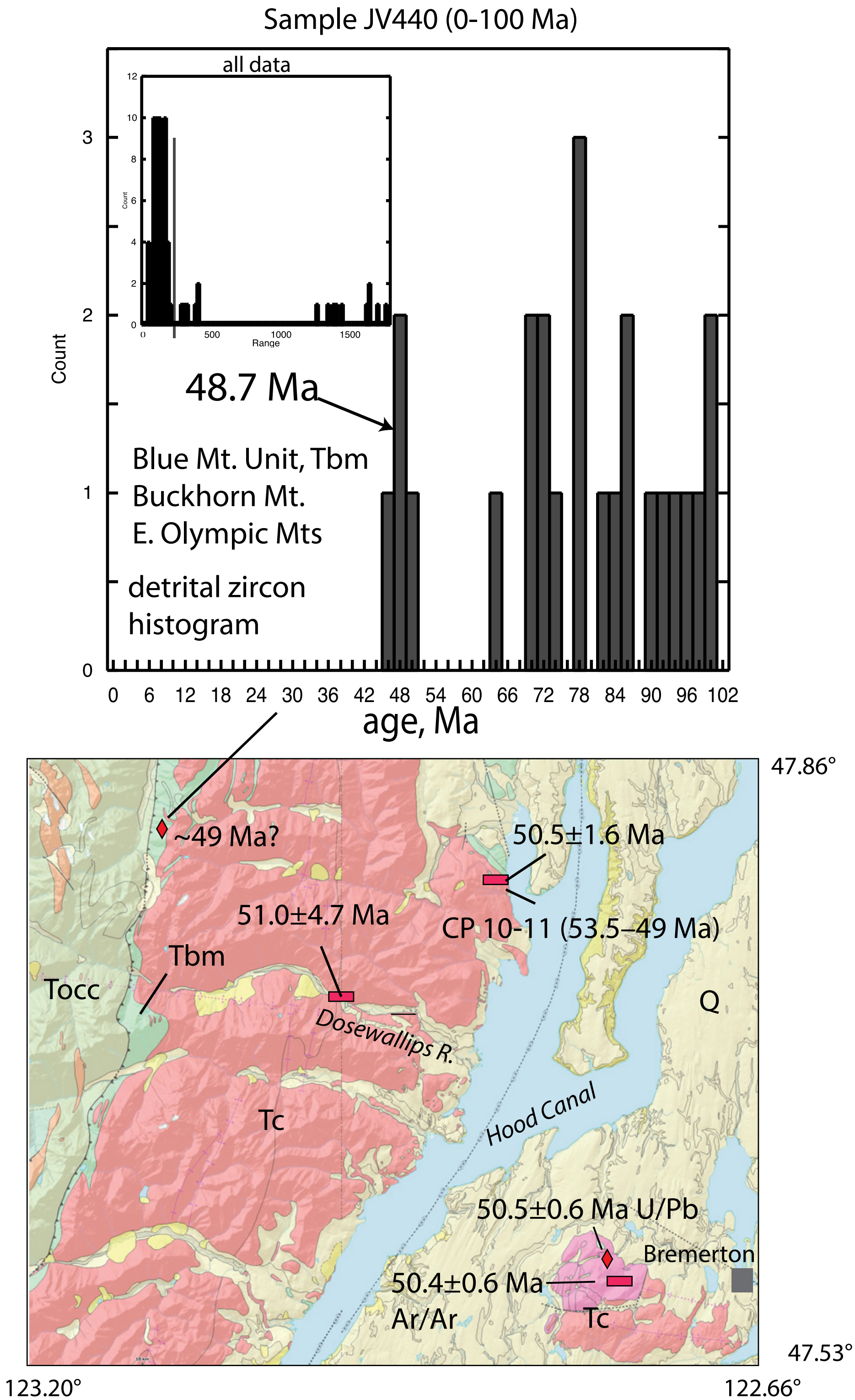

Figure 3. Geologic map showing eastern Olympic Mountains (Mts), Dosewallips River section of Hirsch and Babcock (2009), and U-Pb detrital zircon sample location at Buckhorn Peak; see Figure 1B for location of map. Tbm—Blue Mountain unit turbidites; Tc—Crescent Formation; Tocc—Olympic accretionary complex, where T represents the Tertiary period (informal). Q—Quaternary surficial deposits. A few 49 Ma zircons in age histogram suggest that base of Crescent Formation may be young, not much different than $^{40}Ar/^{39}Ar$ ages from top (red bars). Map from https://fortress.wa.gov/dnr/geology/?Theme=wigm (accessed 8 July 2014).

Siletz Terrane

Newport Area

Snavely and Baldwin (1948) and Snavely et al. (1968, 1976a, 1976b, 1976c) mapped and described the type area of the SRV between Newport and Corvallis, Oregon (Fig. 1). The bulk of the unit consists of submarine tholeiitic pillow basalt, pillow breccia, lapilli breccia, and thin deep-water mudstone interbeds exposed in broad northeast-striking anticlinoria. Although the base of the sequence near Corvallis consists of pillow basalt with mid-oceanic ridge basalt (MORB) affinity, most of the lower tholeiitic unit has higher TiO_2 (2.5%–2.9%) typical of ocean island lavas (Snavely et al., 1968). At Ball Mountain, 30 km north of Newport, the submarine flows are capped by subaerial tholeiitic and alkali basalt. The upper flow sequence contains augite, plagioclase, and olivine phyric flows, shallow-water sandstones, mudflow and debris flow deposits, and abundant bedded lapilli breccia. Large filled lava tubes with carapaces of pillow basalt are characteristic of the submarine part of the upper alkalic unit of the SRV. Interbedded marine mudstones contain nannoplankton referable to coccolith zones CP10 and CP11 (53.5–49 Ma; Bukry and Snavely, 1988), consistent with $^{40}Ar/^{39}Ar$ step-heating ages of 53.3–48.5 Ma (Pyle et al., 2009; Table DR6 in the Supplemental File [see footnote 1]). Both normal and reverse polarities are recognized in the SRV (Simpson and Cox, 1977). The upper part of the SRV interfingers with Kings Valley Siltstone Member (CP10–CP11), and both are unconformably overlain by middle Eocene turbidite sandstone of the Tyee Formation (CP12a and CP12a b; 49–46.5 Ma).

Tillamook Highlands

Eocene basalt composing the Tillamook Highlands has been subdivided into four main units (Wells et al., 1995; Fig. 6). From oldest to youngest, they are: (1) early Eocene SRV, (2) early and middle Eocene Basalt of Hembre Ridge, (3) middle Eocene regional sill complex, and (4) the middle Eocene Tillamook Volcanics. The last two are discussed later; here we focus on the SRV and related rocks.

SRV. The SRV sequence is exposed in the deep canyons of the Trask and Nestucca Rivers, where it consists of submarine tholeiitic and alkalic pillow basalt and pillow and lapilli breccia, overlain by shallow-water fossiliferous basaltic sandstone, and abundant augite-phyric and plagioclase-phyric basalt flows. The SRV in the Tillamook Highlands appears to be the upper part of an ocean island or seamount. The basalts are locally folded, sheared and fractured, with green smectite clay, calcite, zeolite, and

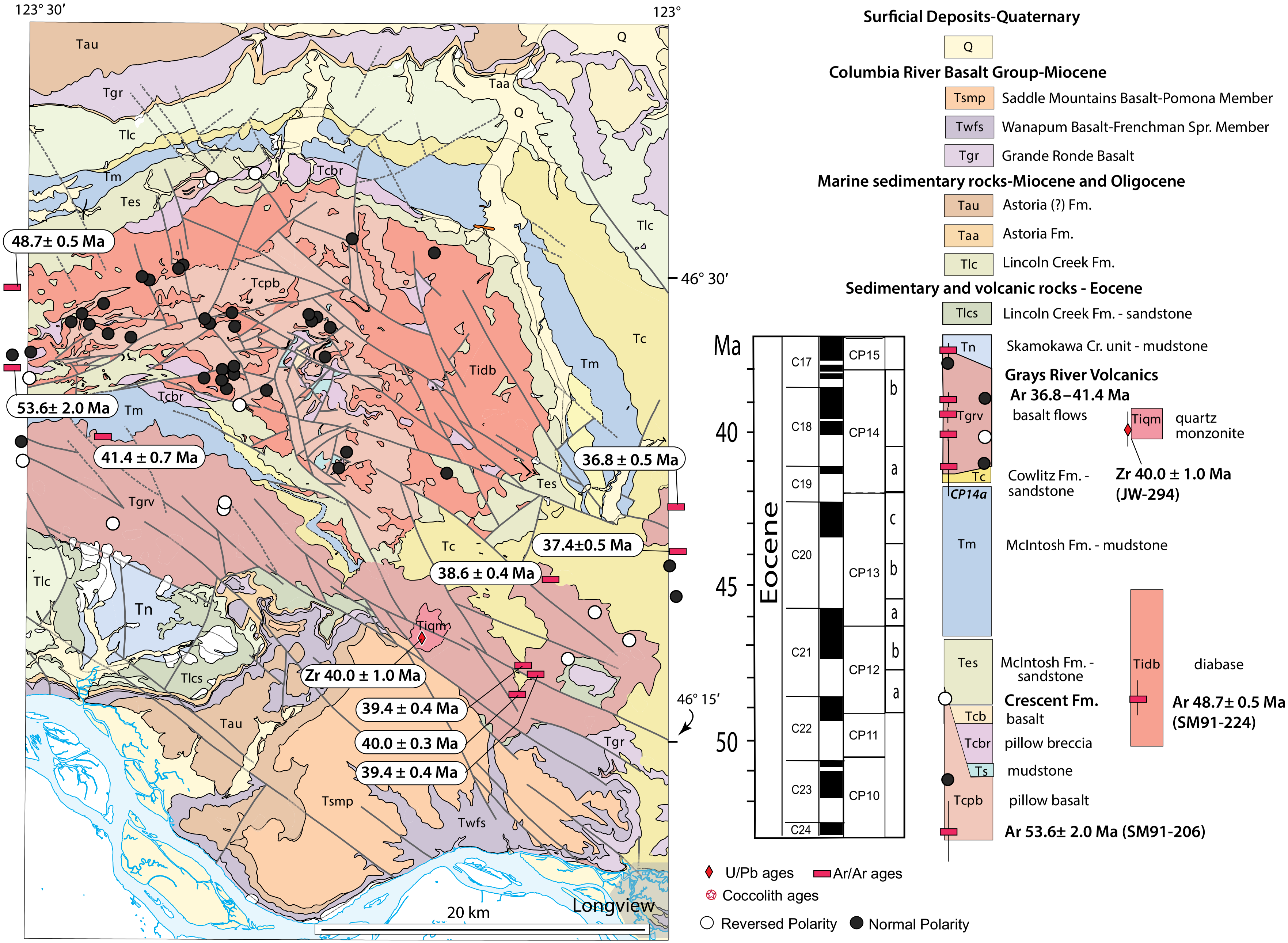

Figure 4. Geologic map of the Willapa Hills (southwest Washington), including locations of sample sites. Geologic column depicts relation of geologic units to Gradstein et al. (2012) time scale. See Figure 1B for location of map. Dated U-Pb and Ar/Ar samples in Grays River volcanics are shown by red diamonds and bars (modified from Wells, 1981; Wells and Sawlan, 2014; Chan et al., 2012).

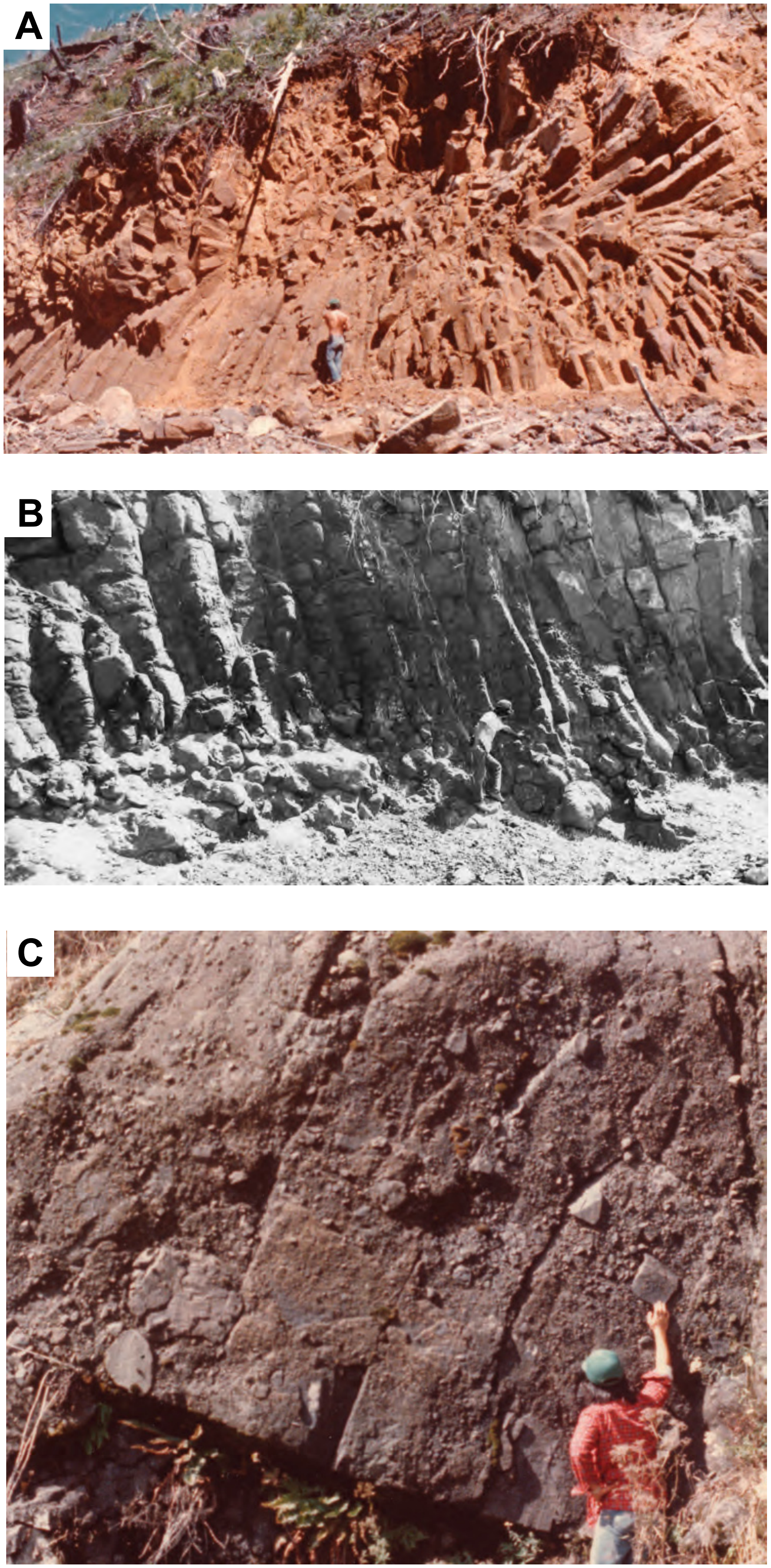

Figure 5. Submarine flows and sills in the Crescent Formation, Willapa Hills (southwest Washington). (A) Giant feeder tube in pillow basalt (unit Tcpb, Fig. 4). (B) Columnar jointed sheet flow with pillowed feet (unit Tcpb, Fig. 4). (C) Submarine basaltic debris flow deposit (unit Tcbr, Fig. 4).

quartz vein and vesicle fillings. Deformation also affects overlying and interfingering deep-water Trask River basaltic turbidite beds, which are locally isoclinally folded.

Nannoplankton from interbeds in the basalt are referable to coccolith zones CP9b, CP10, and CP 11 (54.5–49 Ma), while those from overlying basaltic turbidites are referable to CP10– CP11 (Bukry and Snavely, 1988; Bukry, *in* Wells et al., 1995; Table DR1 in the Supplemental File [see footnote 1]). A U-Pb age from zircons in a tuff bed in the basaltic turbidites gives an age of 52 ± 1 Ma (Figs. 6 and 7A; Table DR2 in the Supplemental File [see footnote 1]). A $^{40}Ar/^{39}Ar$ step-heating age of 50.6 ± 0.8 Ma from pillow basalt in the southern highlands is consistent with the CP and U-Pb ages (Pyle et al., 2009; Table DR6 in the Supplemental File [see footnote 1]). The ages and stratigraphic setting indicate that the Trask River beds are correlative with the Kings Valley Siltstone Member of the SRV near Corvallis and the Umpqua Group near Roseburg. Along the eastern flank of the Coast Range, a faulted anticline in the Gales Creek fault zone exposes subaerial flows of columnar to blocky basalt with red, oxidized flow tops, and an overlying 20-m-thick welded rhyolitic ash flow tuff (Fig. 7A). The tuff is 200 m from the top of the SRV, and zircons from the tuff form a single population with a concordant U-Pb age of 49.0 ± 0.8 Ma (Fig. 8; JW 286, Table DR4 in the Supplemental File [see footnote 1]).

Basalt of Hembre Ridge. An upper sequence of more gently folded, aphyric, tholeiitic pillow basalt overlies the Trask River folded turbidite beds. The Hembre Ridge unit contains filled lava tubes with pillowed carapaces, similar to the upper part of the type SRV and Crescent Formation in the Willapa Hills, and we interpret it as the upper part of the SRV. Chemically, the basalts have MORB affinity, with lower TiO_2 (1.4%–2.0%) and K_2O (0.2%). The upper part of the unit interfingers with very micaceous turbidite sandstone. The sandstone interbeds contain nannoplankton referable to CP zones 12a and 12b (49–46.5 Ma), the same age and mica-rich lithology as the Tyee Formation in the southern Coast Range. Detrital zircon from the Tyee-equivalent sandstone in the Wilson River

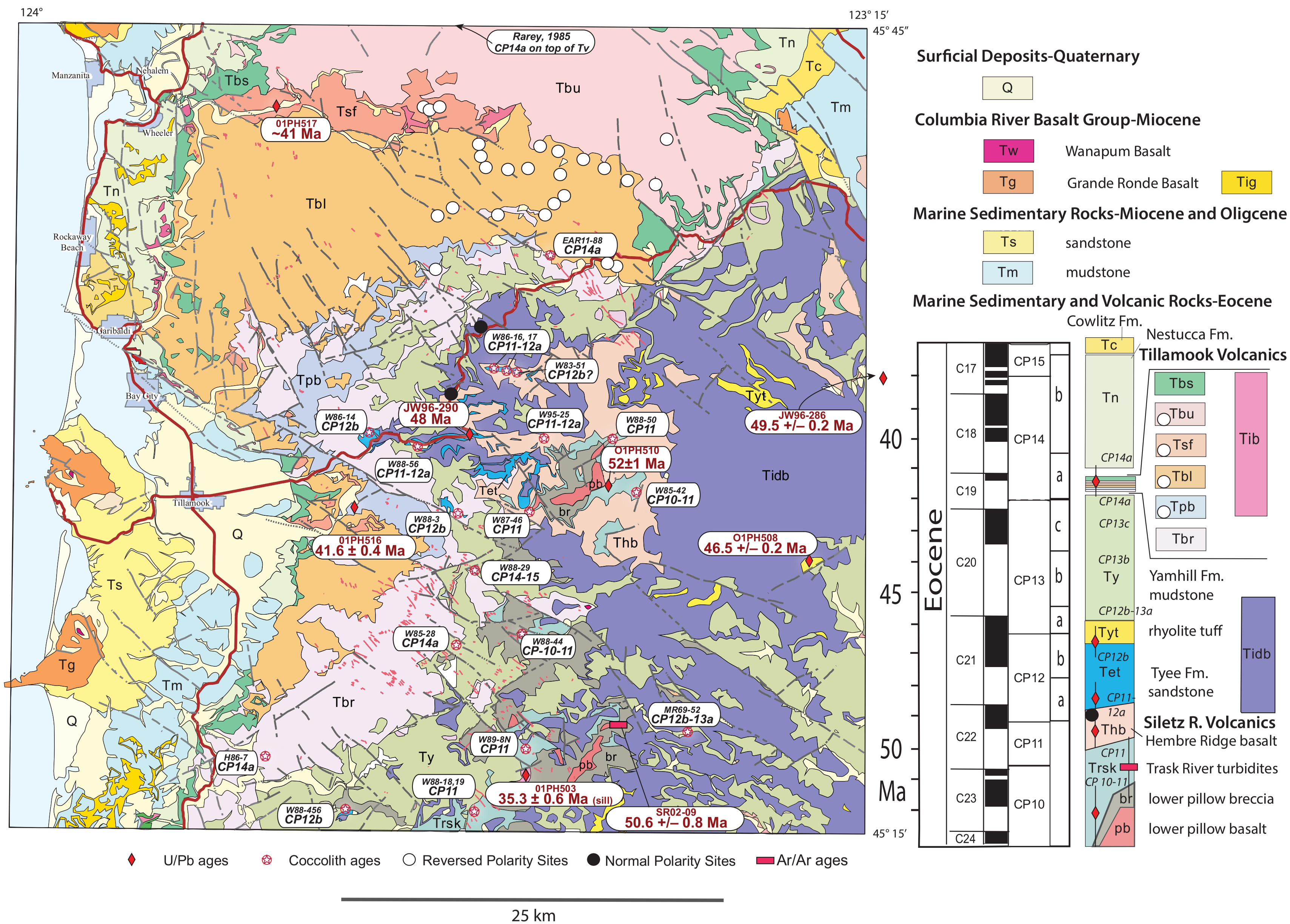

Figure 6. Geologic map of the Tillamook Highlands (Oregon) including locations of sample sites (location in Fig. 1B). Geologic column depicts correlation of geologic units with time scale of Gradstein et al. (2012). Sill complex (purple) effectively separates isolated outcrops of accreted Siletz River Volcanics from broad expanse of postaccretion Tillamook Volcanics. Locations of coccolith samples with CP zone determinations (*italics*) and dated U-Pb samples are shown. Tillamook Volcanics units: Tbs—Fossiliferous basaltic sandstone, Tbu—Upper basalt, Tsf—Dacite and rhyolite flows, Tbl—Lower basalt, Tpb—Pillow basalt, Tbr—Submarine breccia and basaltic turbidites, Tib—Tillamook basalt dikes and sills. Pre-Tillamook units: Tidb—regional basalt sill swarm, Thb—Basalt of Hembre Ridge, br—Submarine breccia of Siletz River Volcanics, pb—pillow basalt of Siletz River Volcanics. From Wells et al., (1995); Bukry and Snavely (1988); this paper. Magnetic polarity is from Magill et al. (1981).

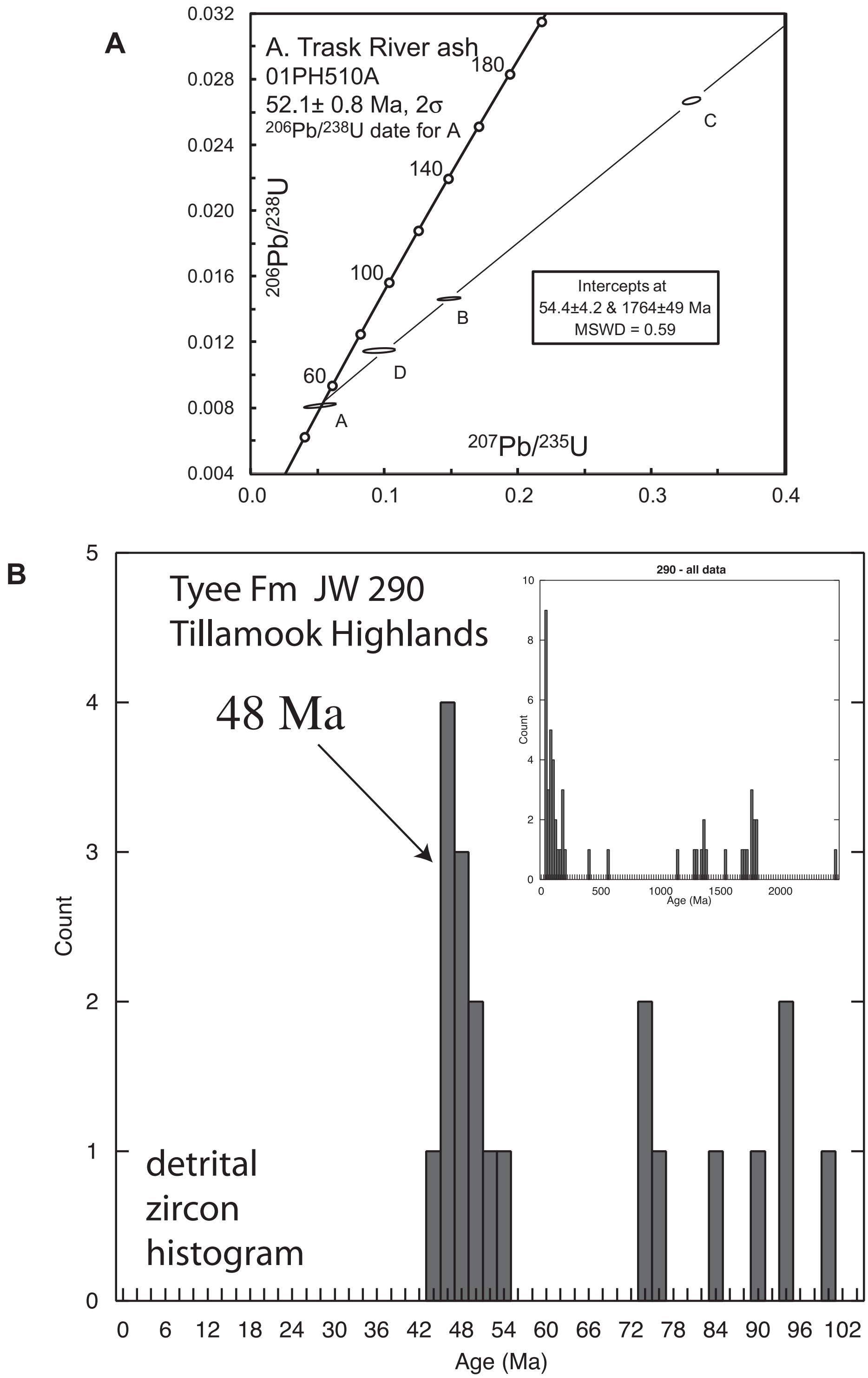

Figure 7. U-Pb ages of Siletz River Volcanics (SRV) and interbedded sediments, Tillamook Highlands (Oregon). (A) 52 Ma Trask River interbeds at top of SRV, Trask River Road. MSWD—mean square of weighted deviates. (B) 48 Ma Tyee Formation. Interbed in basalt of Hembre Ridge, an upper SRV unit.

gives a young U-Pb age peak of 48 Ma, consistent with peak ages derived from 7 samples of Tyee sandstone reported in Dumitru et al. (2013) (Table DR5 in the Supplemental File [see footnote 1]). The consistency probably reflects the forearc basin setting of the Tyee sandstones and nearby volcanic sources. Slope mudstones of the Yamhill Formation (CP13 and CP14a; 47–38 Ma) overlie the Hembre Ridge basalt and the Tyee Formation. We interpret the Hembre Ridge unit as an onlapping seamount, slightly younger than the type SRV, erupted during the late stage of accretion.

Roseburg

We use the term Siletz River Volcanics (SRV) for the submarine basalt exposed beneath the Umpqua Group strata at Roseburg, Oregon, following the usage and correlation of Molenaar (1985), Ryu et al. (1996), and Wells et al. (2000). The SRV in the southern Coast Range crops out in a northeast-striking fold and thrust belt formed along the boundary fault with adjacent Mesozoic terranes (Fig. 9; Diller, 1898; Baldwin, 1974; Wells et al., 2000). Here the SRV consists dominantly of aphyric pillow basalt, with lesser pillow breccia, lapilli tuff, laminated tuff, basaltic sandstone, and mudflow breccia, all tightly folded and thrust faulted (Fig. 9). Interbeds of lithic turbidite sandstone, mudstone, and conglomerate contain chert, limestone, greenstone, plutonic rocks, and metagraywackes derived from the overthrust Early Cretaceous and Late Jurassic Dothan Formation, correlative with the central belt of the Franciscan Complex in California (Blake et al., 1985; Wells et al., 2000). Subaerial flows and interbedded basaltic sandstone containing echinoderms, limpets, and other rocky shoreline species are exposed in the Turkey Hill and Drain anticlines. Subaerial flows are also encountered at ~3.96 km depth, beneath ~2.44 km of pillow basalt in the Sutherlin #1 exploration well. These flows represent one or more ocean islands in the southern part of Siletzia. Basaltic flows from the Roseburg area are dominantly alkalic, locally becoming basanitic and nephelinitic in the Drain area (Pyle, 1988; Wells et al., 2000). Pb, Sr, and Nd isotopic variations show that the SRV mantle source shares similarities with early Columbia River Basalt lavas (i.e., Imnaha and Steens Basalts) and is unlike typical upper mantle MORB sources, such as those that produced the East Pacific Rise and the Gorda–Juan de Fuca–Explorer Ridges (Pyle et al., 2009).

Calcareous nannoplankton from sedimentary interbeds in the core of the Roseburg anticlinorium are assigned to the latest Paleocene (Fig. 9; ca. 57–56 Ma; Table DR1 in the Supplemental File [see footnote 1]), and one site near Sugarloaf Mountain, south of Coquille, Oregon, is assigned to CP8b (56–55 Ma). Flows from the flanks of the uplift that interfinger with conglomerate and mudstone of the Umpqua Group are assigned to the early Eocene CP10 zone

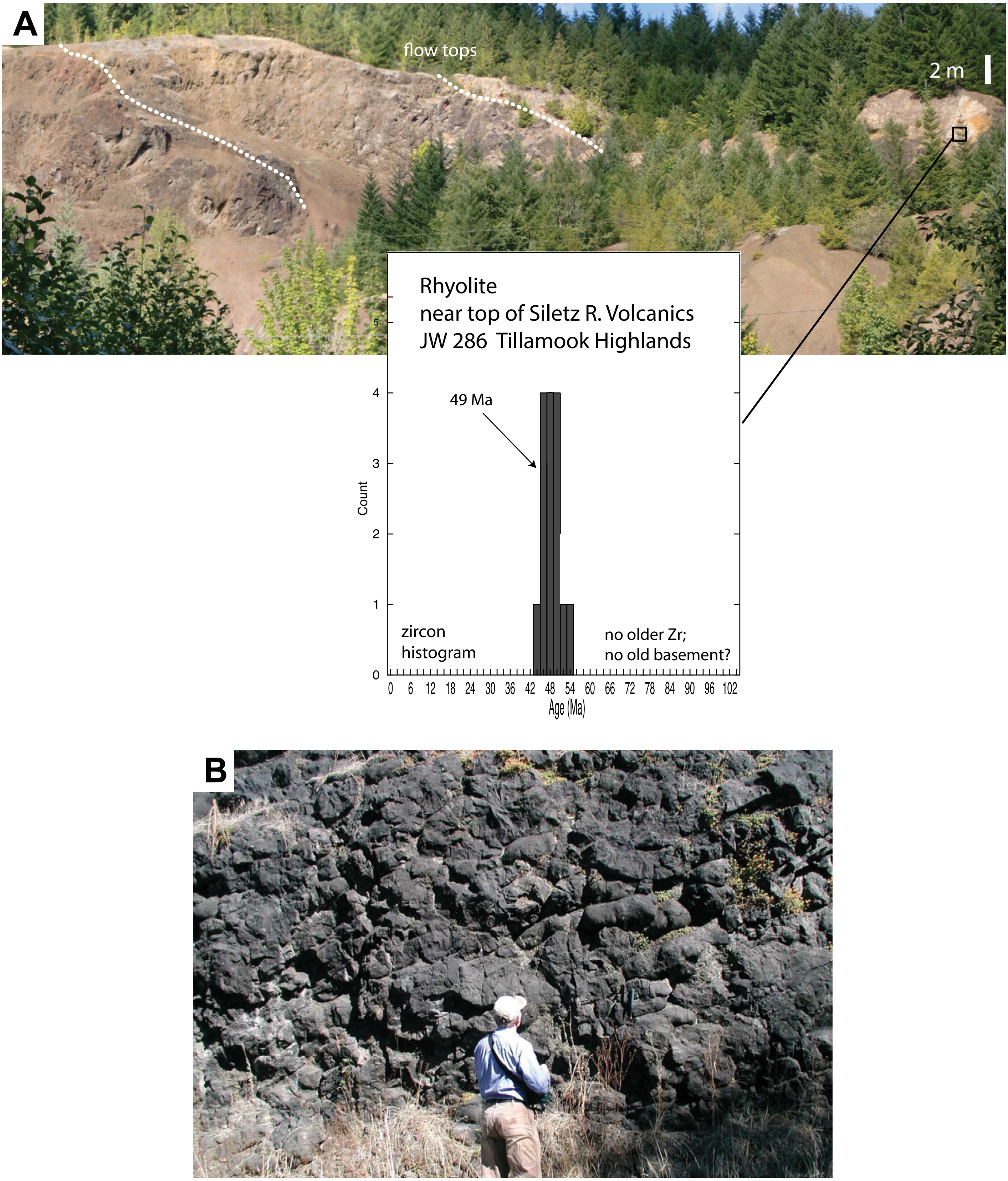

Figure 8. Photos of Siletz River Volcanics (SRV) and sampled units, Tillamook Highlands (Oregon). (A) Rhyolite flow (inset: 49 Ma, U-Pb age on zircons) over basalt, near top of SRV, Carpenter Creek area, eastern edge of map (sample JW96-286, Fig. 6). (B) SRV pillow basalt, Trask River Road (unit pb, Fig. 6).

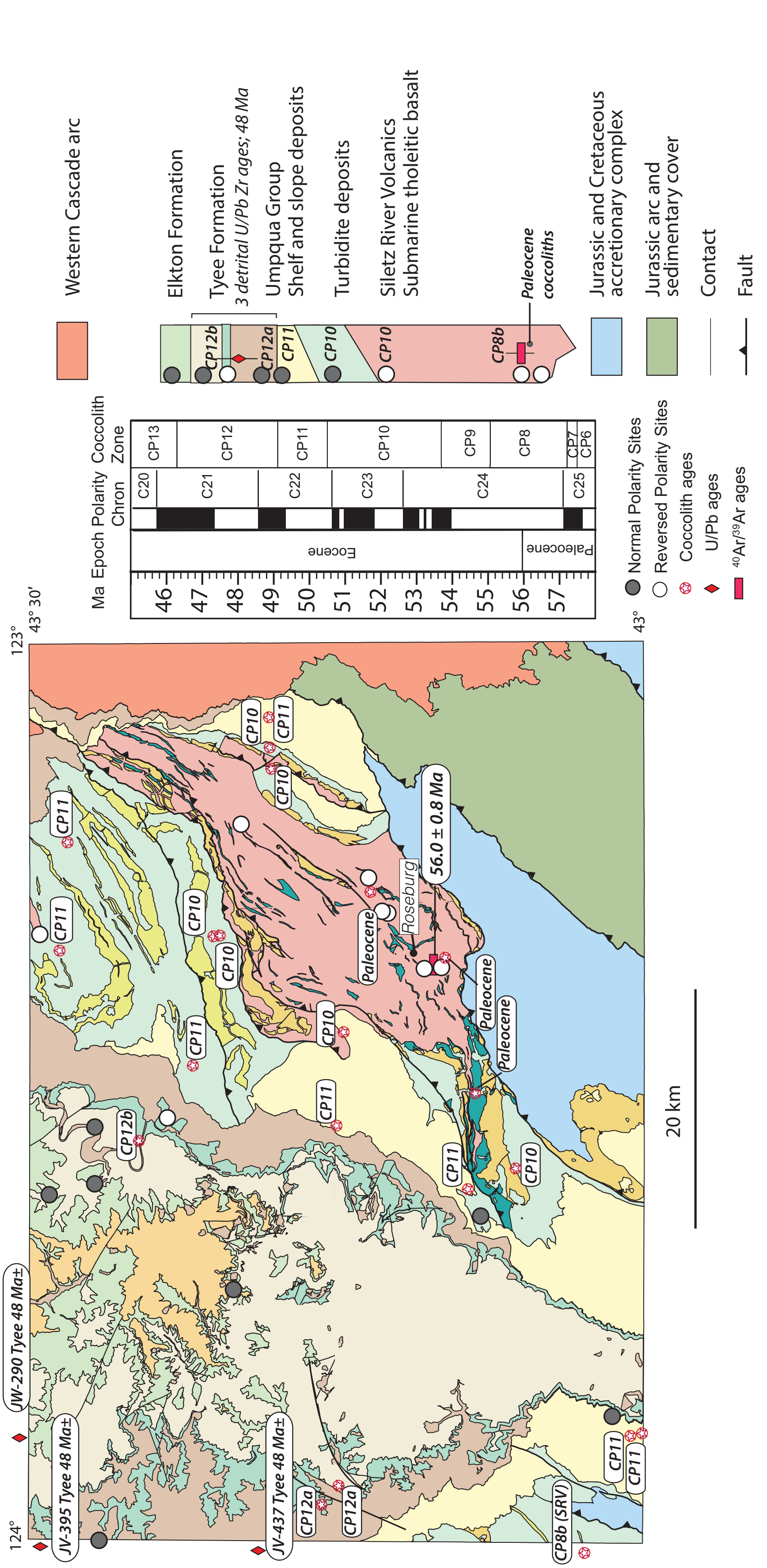

Figure 9. Geologic map of Roseburg (Oregon) 30′ × 60′ quadrangle and correlation of geologic units with time scale of Gradstein et al. (2012). Sample locations are shown on map; see Figure 1B for location of map area.

(53.5–50.5 Ma; Table DR1 in the Supplemental File [see footnote 1]). Ages ($^{40}Ar/^{39}Ar$) of 56.0 ± 0.8 Ma from the Roseburg and Drain anticlinoria and 4 ages of 53 Ma from adjacent uplifts (Pyle et al., 2009; Table DR6 in the Supplemental File [see footnote 1]) are consistent with the CP zone ages.

Yakutat Terrane

The Yakutat terrane currently is outboard of the Fairweather and Chugach–St. Elias faults in the northern Gulf of Alaska (Fig. 1; Plafker, 1987). It is currently being subducted beneath the marginal accretionary complex terranes of southern Alaska (e.g., Eberhart-Phillips et al., 2006; Worthington et al., 2010; Gulick et al., 2013). Most of the terrane is offshore, where its structure is inferred from dredge hauls, well borings, seismic reflection, seismic refraction, and potential field data (Plafker, 1987; Christeson et al., 2010; Worthington et al., 2012). At least 3 km of marine and continental sediments of Eocene through Pliocene age are exposed on land in sparse outcrops (Plafker, 1987). The basal section exposed in the Samovar Hills (Fig. 10) consists of early Eocene pillow basalt and breccia overlain by Eocene slope mudstone, both overthrust by the Early Cretaceous accretionary assemblage of the Yakutat Formation (Plafker et al., 1994). Eocene coal-bearing continental and shallow-marine strata of the Kultieth formation unconformably overlie the thrust package. On the basis of subsurface and marine seismic data, this sequence is inferred to be as much as 15 km thick and to extend offshore to the Transition fault, forming the western boundary of the terrane (Christeson et al., 2010; Worthington et al., 2010).

The pillow basalt is 50–55 Ma and is overlain by middle Eocene mudstone in the Samovar Hills (Plafker, 1987; Plafker et al., 1994). Plafker et al. (1994) hypothesized that the Yakutat terrane migrated ~600 km northward from a location just north of the Queen Charlotte Islands after 35 Ma, whereas Bruns (1983) argued for a more southern source off northern California. Detrital zircon from sandstones of the Kultieth formation have 50–85 Ma U-Pb ages and a dominant fission track cooling age peak of 30–39 Ma (Perry et al., 2009). The formation was derived from an Eocene and Cretaceous nonvolcanic source, likely the Coast Plutonic Complex. Perry et al. (2009) preferred an origin for the terrane north of the Queen Charlotte Islands. A crustal thickness of 24–27 km and velocity structure of the Yakutat terrane are consistent with its origin as an oceanic plateau, with a volume and origin similar to Siletzia (Christeson et al., 2010; Worthington et al.,

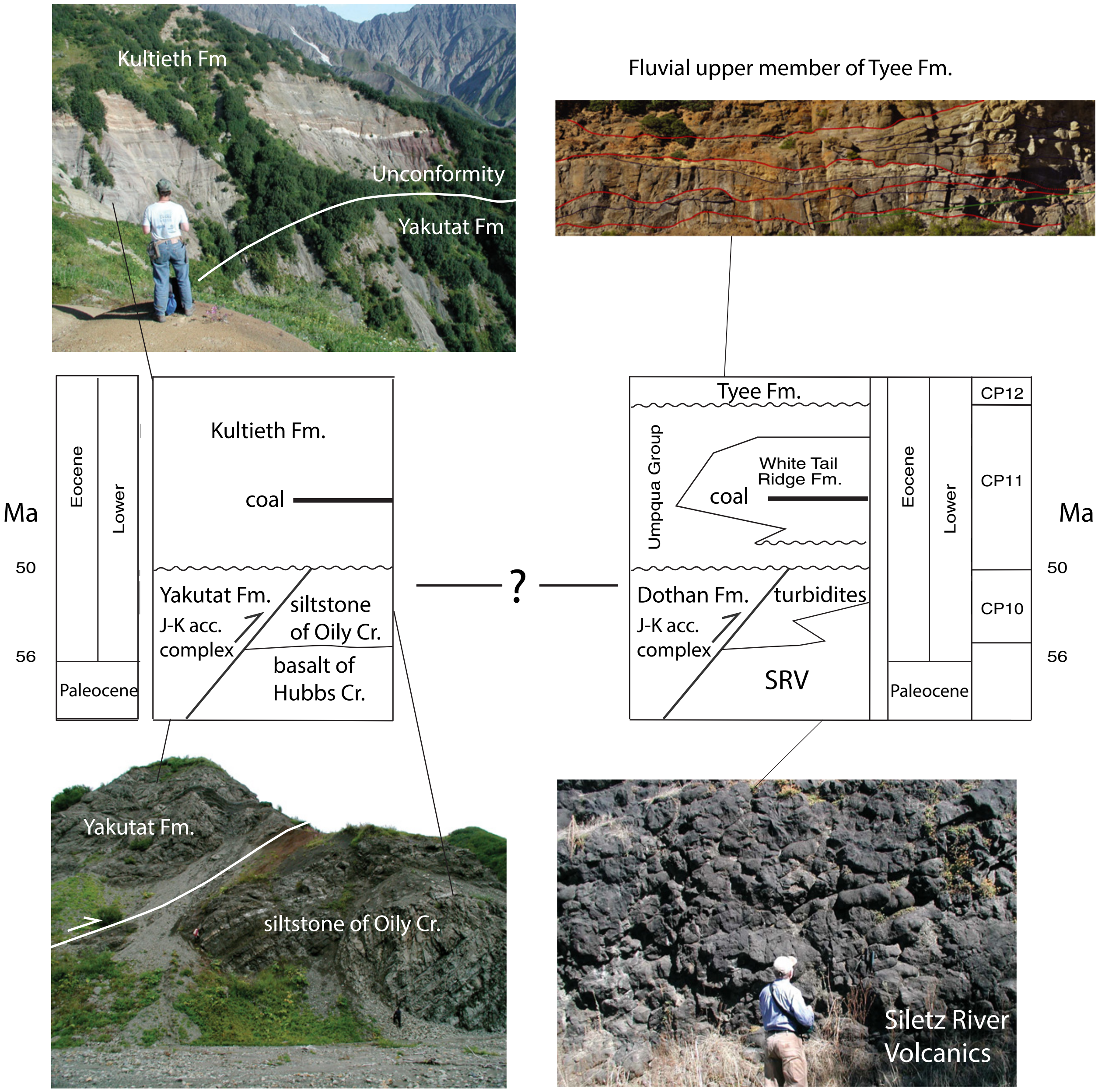

Figure 10. Generalized stratigraphy of Yakutat and Siletzia terranes from Plafker (1987) and Wells et al. (2000). Left side shows Yakutat terrane exposed in the Samovar Hills, a nunatak surrounded by the Malaspina Glacier (Alaska; photos by R. Wells). J-K acc.—Jurassic–Cretaceous accretionary. Upper left photo shows subaerial Eocene Kultieth formation unconformably overlying vertically dipping accretionary complex of Yakutat Formation. Lower left photo shows Yakutat Formation thrust over Eocene marine mudstone of Oily Creek (Cr.). Person below thrust is 2 m tall. Upper right photo shows 10-m high-cliff of fluvial Eocene Tyee Formation (with permission from Santra et al., 2013). Tyee unconformably overlies thrust separating Siletz River Volcanics from overlying Mesozoic accretionary complex of the Dothan Formation. Note that the early history of the Yakutat terrane is very similar to that of Siletzia. Lower right photo shows pillow basalt of the Siletz River Volcanics (SRV).

2012). Collision with North America must have happened in the early Eocene, similar to Siletzia (Worthington et al., 2012), and prior to intrusion by Eocene plutons (Haeussler et al., 2003). The Yakutat basalt basement is chemically similar to the basalts of Siletzia, and Davis and Plafker (1986), Christeson et al. (2010), and Worthington et al. (2012) suggested that Siletzia and the Yakutat basement might have had a common origin. In a later section we examine the possible relation in a northeast Pacific basin plate tectonic reconstruction.

HOOKING SILETZIA UP TO THE GPTS

Systematic geologic mapping and concurrent sampling of sedimentary units for calcareous nannoplankton (e.g., Bukry and Snavely, 1988; Wells et al., 1995, 2000; Table DR1 in the Supplemental File [see footnote 1]) provide a global stratigraphic framework in which to interpret the magnetic polarities, $^{40}Ar/^{39}Ar$ ages of interbedded volcanics, and new U-Pb ages from zircon-bearing volcanic and sedimentary rocks (Tables DR2–DR6 in the Supplemental File [see footnote 1]). We correlate our magnetic polarity, CP zones, and isotopic ages with the GPTS.

For the Roseburg area, we have correlated paleomagnetic polarity data from the SRV (Wells et al., 2000) and onlapping Umpqua Group and Tyee Formation (Simpson, 1977) with nannoplankton CP zones (Bukry and Snavely, 1988; this paper; Table DR1 in the Supplemental File [see footnote 1]; Figs. 2 and 9). Magnetic polarity of the SRV at Roseburg is all reversed, and its CP zones 8b–10 indicate the basalt flows were erupted during Chron 24r and 23r. The $^{40}Ar/^{39}Ar$ step heating ages from 56 to 53 ± 1 Ma (Pyle et al., 2009; Table DR6 in the Supplemental File [see footnote 1]) are all consistent with the CP zones and the magnetic polarity. Sparse paleomagnetic data from the overlying Umpqua Group show normal polarity, consistent with the upper part of its CP11 zone (C21n). Overlying sandstone of the Tyee Formation has been assigned to CP zones 12a and 12b (Bukry and Snavely, 1988; Wells et al., 2000), consistent with its normal-reverse-normal polarity sequence, which we assign to C22n-C21r-C21n. Detrital zircon populations from 7 samples from the Tyee Formation have an age peak of ca. 48–49 Ma (Dumitru et al., 2013; Table DR5 in the Supplemental File [see footnote 1]), which is consistent with its CP12 zone. On top of the Tyee Formation in the central and northern Oregon Coast Range are slope mudstones of the middle Eocene Yamhill Formation, which are assigned to CP13–CP14a (Fig. 6). The Yamhill has a distinctive silicic tuff sequence at its base (Fig. 11A; Snavely et al., 1996; Wells et al., 1995), and zircons we collected from the tuff in the Tillamook area have a concordant U-Pb age peak of 46.5 Ma, consistent with the base of the Yamhill CP zone 13 (46.7 Ma). In Washington, sparse U-Pb and $^{40}Ar/^{39}Ar$ ages from the Crescent Formation are consistent with the calcareous nannoplankton zones and magnetic polarities where available, but do not provide the detail available in Oregon (Fig. 2).

The $^{40}Ar/^{39}Ar$ ages, igneous and detrital U-Pb ages, nannoplankton CP zones, and magnetic polarity zonation for the early and middle Eocene Oregon Coast Range stratigraphic section together correlate remarkably well with the GPTS of Gradstein et al. (2012) (Figs. 2, 4, 6, and 9). Thus, the geochronology and biostratigraphy tied to the GPTS make for an improved analysis of the timing of the magmatic and structural history of Siletzia.

ACCRETION OF SILETZIA: KINEMATICS AND TIMING

At the south end of the Oregon Coast Range, the relations between Siletzia, the terrane boundary fault, the pre-Cenozoic continent, and the sedimentary onlap sequence are well documented (Wells et al., 2000). The geology can be subdivided into four northeast-trending tectonic belts separated by major thrust faults (Fig. 12): (1) the Jurassic Rogue volcanic arc and sedimentary cover; (2) the Jurassic and Early Cretaceous accretionary complex of the Dothan Formation (a central belt Franciscan equivalent); (3) the Roseburg anticlinorium composed of the Paleocene–Eocene SRV basement of the Oregon Coast Range; and (4) the early Eocene Umpqua basin fold and thrust belt.

In the early Eocene, the Mesozoic terranes were thrust over the Siletz terrane, creating the Umpqua basin along the continental margin. Folding and thrusting propagated into Siletzia, creating the Roseburg anticlinorium, which was in turn thrust over the Umpqua basin to produce the northwest-verging Umpqua fold and thrust belt. The Tyee Formation (ca. 48 Ma) and the western Cascade lavas (ca. 35 Ma) were unconformably deposited over the deformed tectonic belts.

Fold and Thrust Belt Marks Collision

The Wildlife Safari fault represents the major suture in the early Eocene between the Late Jurassic–Early Cretaceous accretionary complex and the late Paleocene–Eocene Coast Range terranes (Fig. 12). This suture is perhaps the best candidate for a major fault composing part of an early Cenozoic subduction complex (e.g., Heller and Ryberg, 1983). The mapped trace of the fault is consistent with thrusting, and it juxtaposes Late Jurassic–Early Cretaceous Dothan Formation graywacke and blueschist in the hanging wall against footwall conglomeratic diamict and pebbly mudstone in a 30-m-wide steeply dipping shear zone. However, the overlying mélange of the Dothan Formation is 50 m.y. older than the accretion of Siletzia (Wells et al., 2000). Lower zeolite-smectite facies pillow basalt of the SRV and the coherent, unmetamorphosed sedimentary units in the lower plate have none of the penetrative fabric observed at the top of the much older Dothan accretionary complex, where the rocks are phyllitic or semischistose. Although the Wildlife Safari fault represents the boundary fault at the surface, it is unlikely that the exposed Siletz terrane has been subducted to great depth along it. In Wells et al. (2000) and DuRoss et al. (2002) it was speculated, on the basis of gravity data and shallow burial of the exposed basalt, that the shallow part of Siletzia was partly obducted onto the old margin in the Roseburg area.

Below the thrust, basalts of the SRV are folded into open, northwest-vergent folds, commonly bound on the northwest by thrust faults (Fig. 12). Approximately 37% shortening is indicated by restoration of a cross section normal to the fold belt. Isoclinal folding is common along the thrusts, which generally strike N25–60°E and dip 40–70°SE. Fault slip directions trend 285°–315°, indicating northwest to slightly right-oblique directed thrusting (Fig. 12). A channel of Bushnell Rock conglomerate is repeated six times along the North Umpqua River by a series of thrusts, indicating no significant strike-slip motion during thrusting (Wells et al., 2000).

Accretion Complete 50.5–49 Ma

Continental, coal-bearing deltaic sediments of the early Eocene White Tail Ridge Formation (Umpqua Group) onlap the deep-water pillow basalt of the SRV (Fig. 9). Nannoplankton from deep-water strata that interfinger with the SRV are assigned to CP10, whereas nannoplankton from mudstone overlying the coal-bearing White Tail Ridge sandstone are assigned to CP11 (Table DR1 in the Supplemental File [see footnote 1]). The onlap of continental strata thus occurred between 50.5 and 49.0 Ma, during CP11 time, and ~3 m.y. after eruption of the youngest dated basalt at Roseburg. Folding and thrusting locally continued through CP11 time, but ended before deposition of the basal Tyee Formation during CP12a time (49–48 Ma). SRV magmatism continued in the northern Oregon Coast Range into CP12 time (49–46 Ma).

The sedimentary onlap records the end of the collision process, with the basal Bushnell Rock conglomerate recording uplift and erosion of the Mesozoic continental margin during collision (Heller and Ryberg, 1983). Conglomerate in the upper part of the SRV indicates that the process was underway by CP10 time (53.5 Ma) and possibly earlier. The initiation of collision is more difficult to estimate, as there is a 50 m.y. time gap between the youngest rocks in the Dothan accretionary complex (Whitsett limestone blocks, Albian–Cenomanian, 133–94 Ma; Blake et al., 1985) and the oldest rocks in the SRV (56 Ma). Part of the margin may have been removed by subduction erosion during the collision process (e.g., Scholl and von Huene, 2010).

The structural and thermal history of accretion at the southern end of Siletzia at Roseburg is quite different from the history inferred for the suture exposed along the Leech River fault on Vancouver Island (Fig. 2). Presumed lower plate strata of the Umpqua basin have low

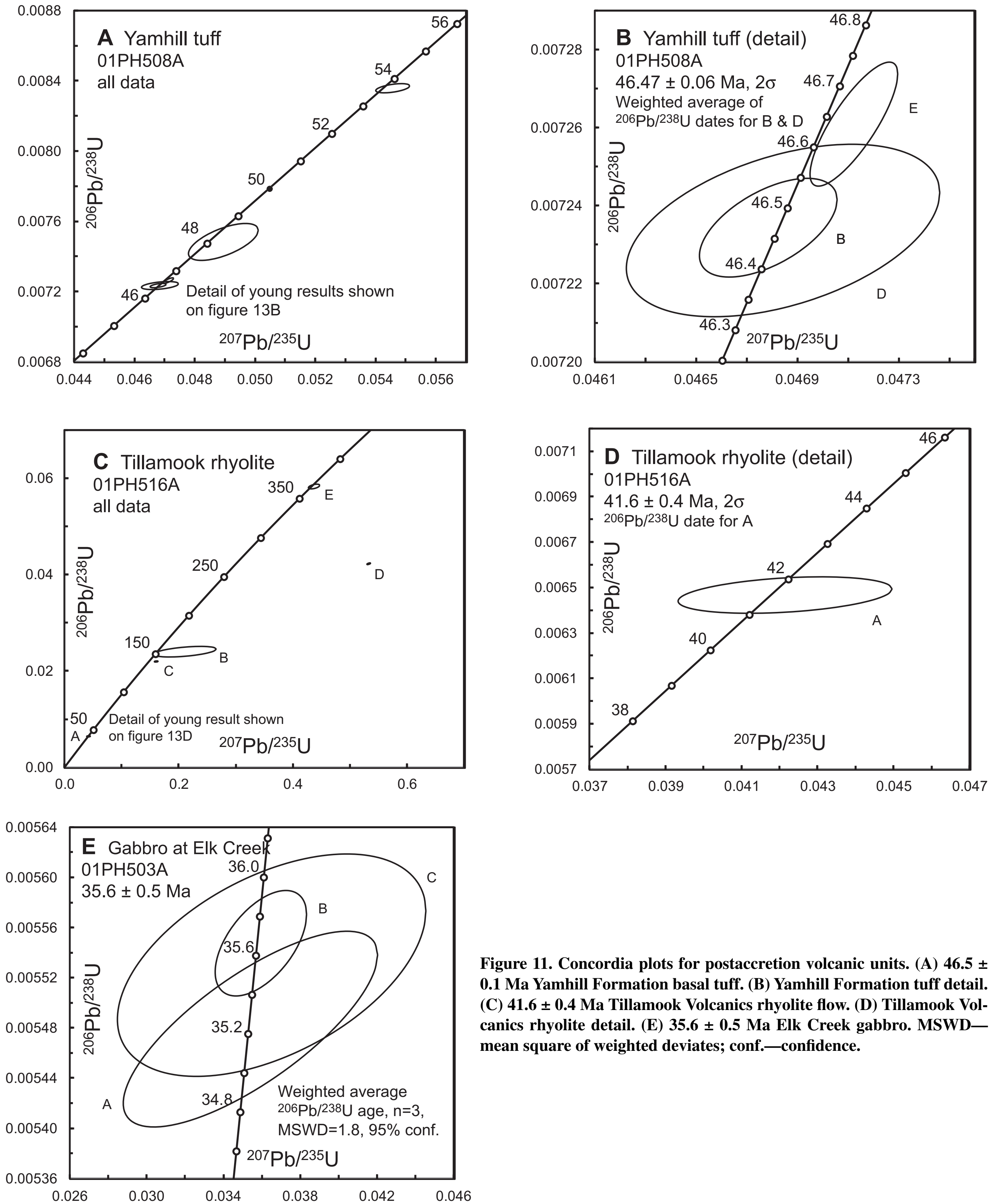

Figure 11. Concordia plots for postaccretion volcanic units. (A) 46.5 ± 0.1 Ma Yamhill Formation basal tuff. (B) Yamhill Formation tuff detail. (C) 41.6 ± 0.4 Ma Tillamook Volcanics rhyolite flow. (D) Tillamook Volcanics rhyolite detail. (E) 35.6 ± 0.5 Ma Elk Creek gabbro. MSWD—mean square of weighted deviates; conf.—confidence.

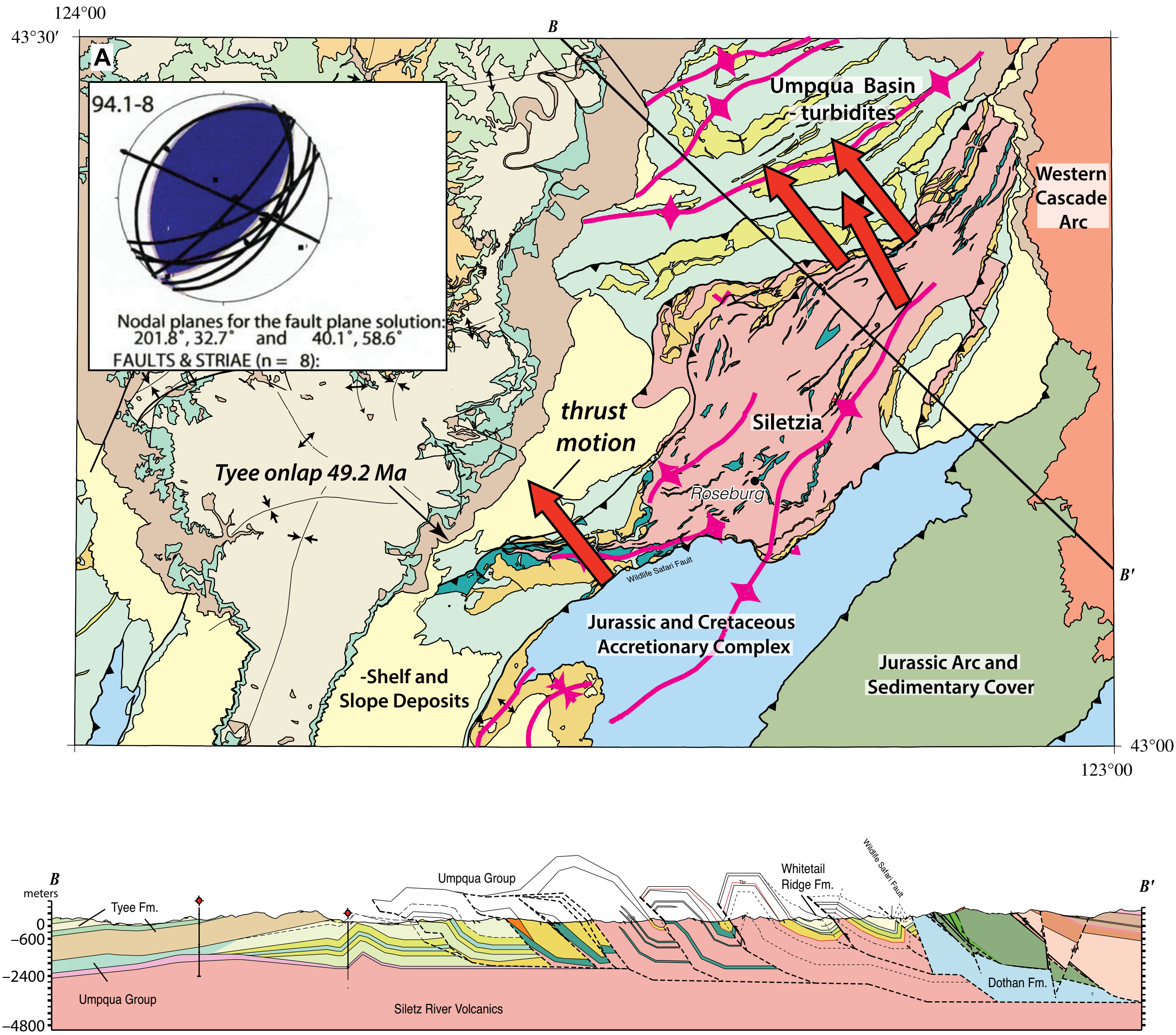

Figure 12. Fold and thrust belt kinematics, Roseburg (Oregon) quadrangle. Geologic units as in Figure 8. Siletzia is thrust beneath old Mesozoic accreted terranes. Red arrows show thrust slip directions derived from slickenlines on the faults. Composite focal mechanism (inset) indicates little or no strike-slip motion during slip (plotted using FaultKin 4; see Allmendinger et al., 2012; for latest version, FaultKin 7, see http://www.geo.cornell.edu/geology/faculty/RWA/programs/faultkin.html). Folds are parallel to precollision margin. B–B′ is a restorable cross section through the fold and thrust belt that accommodates ~37% shortening.

vitrinite reflectance values (Ryu et al., 1996) indicating relatively shallow burial, and the smectite clay–zeolite assemblage in the SRV also appears consistent with shallow burial. This contrasts with lower greenschist facies of the lower plate Metchosin igneous complex on Vancouver Island and the 45 Ma cooling age of the Leech River schist in the upper plate, presumably as a result of uplift during accretion of the Crescent terrane (Groome et al., 2003). No sedimentary onlap of the Metchosin igneous complex is recorded until deposition of the Carmanah group in the late Eocene and Oligocene.

Accretion, Rotation, and the Formation of the Columbia Embayment

The accretion of Siletzia into the Columbia embayment could indicate a possible relation between accretion and formation of the embayment (e.g., Schmandt and Humphreys, 2011). In contrast, Wyld et al. (2006) suggested that the embayment formed in Late Cretaceous and early Cenozoic time by 450–900 km northward migration of northern Cordilleran terranes, leaving an embayment behind. Given postaccretion rotation of Siletzia and late Cenozoic opening of the Basin and Range, at least the southern limb of the embayment has been rotated clockwise during the Cenozoic (e.g., Irving 1964). Here we examine the relation between rotation and formation of the embayment.

Eocene rocks of the Oregon Coast Range have been rotating clockwise at 1.19°/m.y. since at least 50 Ma (Simpson and Cox, 1977; Beck and Plumley, 1980; Magill et al., 1981; Grommé et al., 1986; Wells et al., 1998; McCaffrey et al., 2007). The SRV is rotated more than 70°, and successively younger strata are rotated lesser amounts. At Roseburg, the 56–53 Ma reversed flows of the SRV are rotated 79° ± 12.5° clockwise (Wells et al., 2000). The relatively undeformed Tyee Formation, which onlaps both the Mesozoic margin and the Umpqua fold and thrust belt that formed during accretion of Siletzia, is rotated 67° ± 14.5° (Simpson and Cox, 1977; Grommé et al., 1986). Thus, most of the measured paleomagnetic rotation postdates accretion of Siletzia at Roseburg (Fig. 13). This observation and the lack of younger accretion-related deformation in the Tillamook area (Fig. 6) are inconsistent with earlier tectonic models that require large rotation (>50°) of an Oregon Coast Range–sized Siletz terrane during oblique collision (e.g., Magill et al., 1981). However, the uncertainties are large enough to permit some collision-related rotation of the SRV (cf. McCrory and Wilson, 2013). The SRV at Roseburg is rotated 12° more than the onlap assemblage, and Mesozoic trends on southernmost Vancouver Island were rotated counterclockwise 20° during collision of Siletzia ca. 45 Ma (Johnston and Acton, 2003).

We can infer the shape of the Columbia embayment at the time of accretion from the northeast-striking, collision-related fold belt at Roseburg that is subparallel to the northeast strike of the boundary fault and Mesozoic marginal terranes. Removing the 67° ± 14° rotation of the Tyee onlap reconstructs the orientation of the folds and presumably the margin at Roseburg prior to folding. The original trend of the folds was ~330° ± 14°, and a similar back rotation of early formed folds throughout Siletzia (Wells and Coe, 1985; Wells, 1989b) indicates that the orientation of the backstop for the exposed part of Siletzia formed a less embayed margin than that inferred from the Mesozoic orocline (Fig. 13B). Approximately 16° of the rotation of the orocline at Roseburg is related to post–16 Ma Basin and Range extension (Colgan and Henry, 2009; Wells and McCaffrey, 2013). However, the unconformity at the base of the Western Cascades volcanic arc cuts across the Mesozoic trends and is rotated ~30° (Magill and Cox, 1980). Thus, some rotation of the fold and thrust belt and precollision margin occurred between Tyee Formation (48 Ma) and Western Cascades time (20–30 Ma). We suggest that distributed shear, similar to what is happening today (McCaffrey et al., 2007) along the obliquely convergent margin, is responsible for postaccretion rotation in excess of Basin and Range-related rotation.

The present extent of Siletzia west of the Cascade arc may represent only a portion of a larger terrane that began collision much earlier. Late Cretaceous and early Cenozoic folding and thrusting of the Cowichan fold belt and continued folding of the early Eocene Chuckanut Formation east of Vancouver Island may be due to initial collision of a larger Siletzia. Likewise, the dextral motion of the Straight Creek fault and other Cordilleran dextral faults in Late Cretaceous and Paleogene time (Ewing, 1980; Wyld et al., 2006) may be due to oblique collision of Siletzia into the Columbia embayment (McCrory and Wilson, 2013) and perhaps collision of the Yakutat terrane farther north. Although Siletzia is not exposed east of the Coast Range, a remnant of Siletzia is hypothesized to extend eastward beneath the Mesozoic terranes that compose the basement of the southern Columbia Plateau in eastern Washington (Schmandt and Humphreys, 2011).

POSTACCRETION MARGINAL RIFTING AND MAGMATISM

Middle Eocene Sill Complex

Following the accretion of Siletzia, the nature of deformation and magmatism in the developing forearc changed dramatically. The first event was the regional emplacement, from the central Oregon Coast Range to the Olympic Mountains, of a low-K, MORB-like sill complex into the upper SRV and Tyee and lower Yamhill Formations, immediately after suturing of Siletzia to Oregon.

The regional sill complex consists of tholeiitic basalt, diabase, and gabbro that is widespread in the Oregon Coast Range north of Newport and is well exposed south of the Wilson River Highway (State Route 6) in the Tillamook Highlands (Figs. 6 and 14B). The sill complex is also well exposed in the eastern Willapa Hills in southwest Washington (Fig. 4). Sills preferentially intrude along the upper contact of the SRV and complexly interfinger with the basalt of Hembre Ridge and the Tyee Formation in the Tillamook area. The sills are chemically similar to the Hembre Ridge unit and have MORB affinity (Moothart, 1993). Some of the sills are pillowed; others are layered, with well-defined banding of zeolite amygdules and microphyric plagioclase (Fig. 14B). Rare exposures indicate that the layering is concentric around the margins of intrusions and lacking in the centers, suggesting a type of flow banding. Dikes of the same age and composition are exceedingly rare; very few have been recognized throughout the Coast Ranges of Oregon and Washington.

The sills are not easily dated because they have low K_2O (0.2%), are commonly zeolitized, and their intrusion has destroyed most of the microfossil assemblages in the intervening sediments. Further complications arise because the sills can be indistinguishable from sheet flows in the Hembre Ridge unit, and later sills related to Tillamook and Cascade Head volcanism are locally interleaved with the middle Eocene complex (e.g., 35 Ma Elk Creek sill, Fig. 11E). A $^{40}Ar/^{39}Ar$ age of 48.7 Ma from a sill from the Willapa Hills is the only isotopic age available (Moothart, 1993). The sills intrude the tuffaceous unit composing the basal Yamhill Formation. U-Pb ages from the tuff give a concordant age of 46.5 ± 0.1 Ma (Fig. 11A), consistent with CP13a zone (46 Ma). Numerous dikes that feed the overlying Tillamook Volcanics (ca. 42 Ma) cut through the sills.

Dikes coincident with sill intrusion are exceedingly rare. Intrusion apparently occurred beneath the seafloor, shortly following accretion of Siletzia to the continent. The sills may represent a change in forearc stress state following accretion. In Oregon, the sills postdate final suturing by 2–5 m.y. and could be related to formation of the new subduction zone by extension of the upper plate toward the new trench (Gurnis et al., 2004).

Tillamook Magmatic Episode

The second major postaccretion event is marked by normal faulting, bimodal high-TiO_2 basalt-rhyolite magmatism, and regional dike swarms in the forearc. This regional rifting event started ~8 m.y. after accretion in the central Oregon Coast Range and is recognized as far north as the Willapa Hills in Washington (Figs. 2 and 4). The episode is named for the Tillamook Volcanics, the most voluminous of the basaltic accumulations, exposed in the Tillamook Highlands, northern Oregon Coast Range (Fig. 6). Included in this episode are the Yachats Basalt and Cascade Head basalt along the Oregon coast, and the Grays River volcanics in the Willapa Hills, Washington (Fig. 4). Porphyritic subaerial basalt flows dominate in the larger Tillamook center (Fig. 14A). Pillow basalt and submarine breccias are common in the lower parts, and some lapilli tuffs are very porphyritic, with megacrysts of augite as much as 1 cm across (Wells et al., 1995) and plagioclase as much as 10 cm long (Wells, 1989a). Most of the volcanic centers are capped by basaltic sandstone and boulder conglomerate eroded from the edifices and containing oyster, limpet, and other shallow-water fossils. Ultimately, the volcanoes were onlapped by deep-water slope

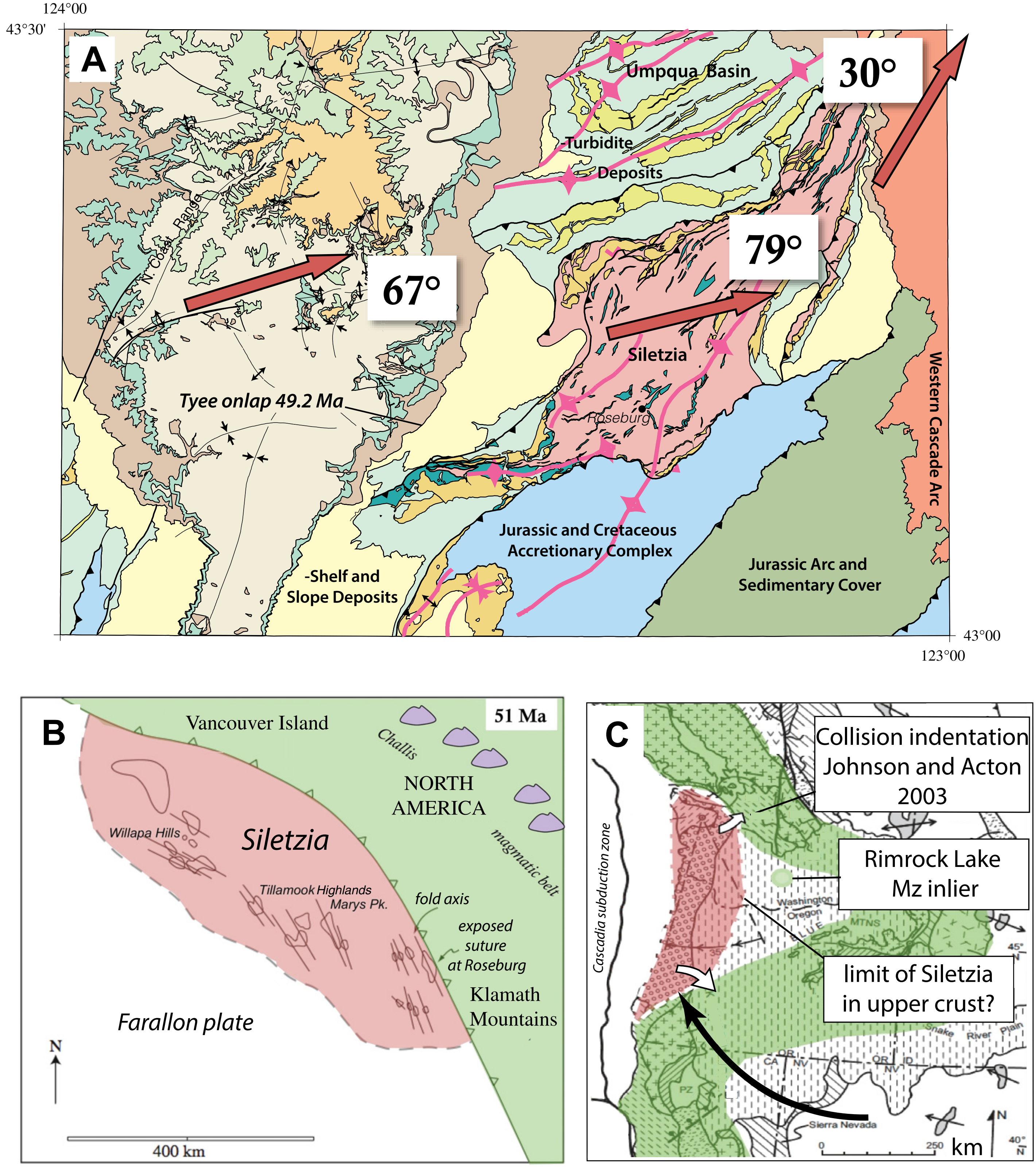

Figure 13. (A) Clockwise paleomagnetic rotations, Roseburg (Oregon) area. Most rotation postdates accretion-related folding. (B) Restored Paleocene margin after removing 67° ± 14° postaccretion rotation of Tyee onlap. (C) Siletzia fills western part of Columbia embayment in Mesozoic orogen (green overprint on terranes, modified from Dickinson (2004). White arrows show indentation from collision of Siletzia; black arrow shows rotation from Basin and Range extension. Mesozoic (Mz) rocks of Rimrock Lake inlier limit eastward extent of Siletzia in the shallow crust, although it may underplated in the deep crust.

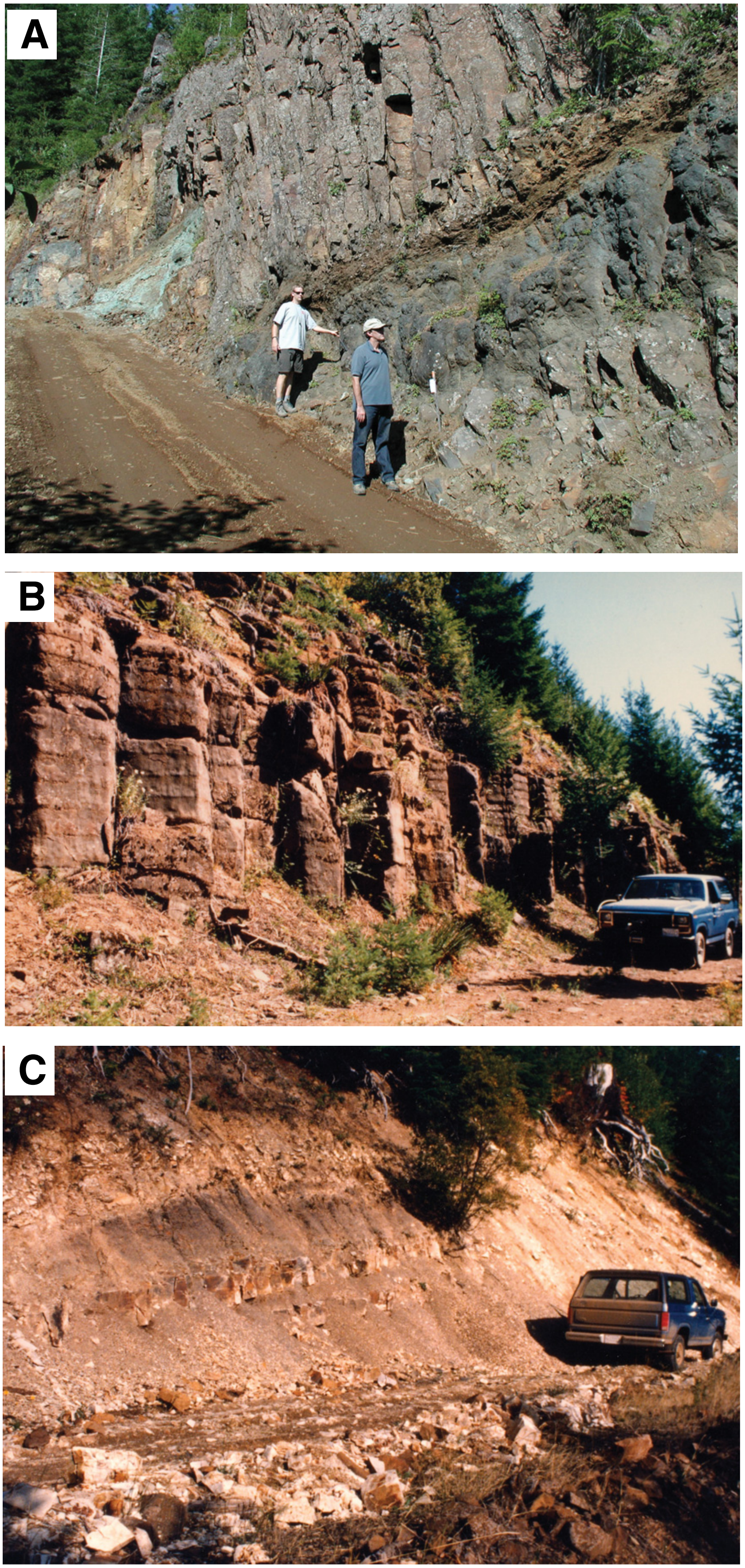

Figure 14. Photos of postaccretion rocks. (A) Subaerial flows of Tillamook Volcanics south of Triangulation Peak, Oregon (unit Tbl, Fig. 6). (B) Regional basalt sill complex, upper Tualatin River gorge, Oregon, intruded into tuff beds and all older units (unit Tidb, Fig. 6). (C) Tuff at base of Yamhill Formation on ridge above North Fork Trask River, Oregon (unit Tyt; CP12b–13a fossil zone; 46.5 ± 0.5 Ma U-Pb age, Fig. 6).

mudstones, indicating subsidence after a short pulse of volcanism.

These volcanic centers are dominated by high TiO_2 (2.5%–3.5%) tholeiitic and alkalic basalt, and are bimodal, with rare rhyodacite and rhyolite. Major element and trace element chemistry by Snavely and MacLeod (1974), Phillips et al. (1989); Barnes and Barnes (1992), Davis et al. (1995) Parker et al. (2010), and Chan et al. (2012) characterized the flows as enriched (E) MORB and ocean island basalt (OIB) lavas. Parker et al. (2010) and Chan et al. (2012) suggested that the Yachats, Cascade Head and Grays River volcanics may have been sourced in the asthenosphere beneath the Farallon plate, possibly from a plume or slab window source.

In the Tillamook volcanic center, the volcanic sequence is tilted northward toward the synclinal trough forming the lower Columbia River valley (Fig. 1). The northward tilt exposes a cross section of the volcanic edifice, which is built on deep-marine slope mudstone of the Yamhill Formation (Fig. 6). A coarsening-upward, 2-km-thick sequence of basaltic siltstone, sandstone, graded lapilli breccia, pillow breccia, and pillow basalt records the growth of an oceanic edifice to sea level (Fig. 6). Subsequent eruptions built a subaerial shield ~3.4 km thick, locally capped with dacite and rhyolite flows (Wells et al., 1995). The oldest volcano in the Tillamook complex has a diameter of 50 km and a volume approaching 4×10^3 km^3. The basalt flows are commonly very porphyritic, and are locally cumulate, with as much as 40% plagioclase, clinopyroxene, and olivine phenocrysts. Overlying the lower shield is a 3-km-thick sequence of shield-building lapilli breccia, pillow basalt, and subaerial basalt that offlap to the north (Fig. 6), toward the slightly younger Grays River volcanics in southwest Washington (Fig. 2).

Isotopic Ages and CP Zones of Postaccretion Magmatism

The submarine flows and breccias of the Tillamook Volcanics interfinger with and overlie Yamhill mudstone. Three Yamhill localities beneath or within submarine Tillamook Volcanics contain nannoplankton assigned to CP14a (42–40.5 Ma; Table DR1 in the Supplemental File [see footnote 1]). The top of the Tillamook Volcanics is overlain by slope mudstone that also contains nannoplankton referable to CP14a (Rarey, 1985), limiting the major portion of the volcanic pile to a 1.5 m.y. time span. Paleomagnetic data from this sequence are entirely reversed (Magill et al., 1981), and a U-Pb age on zircons from a rhyolite flow near the top of the sequence gives an age of 41.6 ± 0.4 Ma (Figs. 11B, 11C), consistent with the CP zone and the inferred short polarity interval, probably Chron 19r. Earlier K/Ar ages from the Tillamook area span an age range of 46–42.7 Ma, but are not sufficiently precise to determine the duration of volcanism (Magill et al., 1981). Isotopic $^{40}Ar/^{39}Ar$ ages from the Yachats (36.9 Ma), Cascade Head (34.2 Ma), and Grays River (41–37 Ma) centers decrease to the north and south, away from the Tillamook center (this paper; ages summarized in Chan et al., 2012; Fig. 2), consistent with the geologic evidence of offlapping shields to the north. These centers are of mixed polarity (Simpson and Cox, 1977; Wells and Coe, 1985), and the Yachats and Cascade Head lavas are interbedded with mudstone containing nannoplankton referable to CP15 (38–34.5 Ma; Table DR1 in the Supplemental File [see footnote 1]). One of the intrusions we sampled in the Yamhill Formation, a gabbro at Elk Creek, had a concordant U-Pb age from zircons of 35.6 ± 0.5 Ma, apparently related to the later stages of the Tillamook eruptive episode (Fig. 11E).

The lavas of the Tillamook episode were erupted during regional extension of the Cascadia forearc. The lavas are interbedded with continentally derived coal-bearing strata, and farther east the coal-bearing units are interbedded with andesite flows and breccias of the early arc (Tukwila and Northcraft Formations in Washington, and lower Western Cascades; Fig. 2). The arc lavas indicate that subduction was well established by Tillamook time, although none of the Coast Range lavas appears to be magmatically related to subduction (e.g., Barnes and Barnes, 1992; Chan et al., 2012; Pyle et al., 2009).

Regional Dike Swarms Feeding the Tillamook Episode

Each volcanic center of the Tillamook episode is sourced from west-northwest–trending dike swarms, which crop out from south of Eugene to the Willapa Hills, Washington, a distance of 250 km. Thousands of dikes make up the dike swarms, and they have a preferred orientation of 303° ± 2.1°. Dike orientations are plotted in Figure 15, and we have removed the 46° clockwise tectonic rotation recorded by Tillamook flows (Magill et al., 1981: Grommé et al., 1986). The resulting trend of 257° indicates north-northwest–south-southeast margin-parallel extension during intrusion. Parallel to the dike swarms are normal faults, including those that form the trapping faults at the Mist gas field in northwest Oregon. These normal faults were formed at about the same time as the dikes, and they are overlain by a regional unconformity at the base of the Cascade-sourced tuffaceous marine mudstone of the Keasey Formation in Oregon (ca. 37 Ma; Fig. 2; Niem and Niem, 1985). The unconformity marks the end of major extension and forearc magmatism, although emplacement of small volumes of strongly alkalic and iron-rich magmas continued for another 5 m.y. The eruption of camptonite flows and intrusion of nepheline syenite in the central Oregon Coast Range at 34.6 Ma were approximately contemporaneous with the eruption of the Cascade Head volcanics at 34.2 Ma, and the flows appear to be lesser partial melts of the Cascade Head and Yachats sources (Oxford, 2006; Parker et al., 2010). Intrusions of ferrogabbro between Eugene and Tillamook have been dated by Ar/Ar as 32.46 ± 0.24 Ma (Mary's Peak and other intrusive bodies in Oxford, 2006).

Overall, the Tillamook magmatic episode marks a rejuvenation of magmatism in the Coast Range during a period of regional margin-parallel extension 42–34 Ma. Large volumes of magma were erupted and intruded in the first 2 m.y.; this decreased dramatically, and minor alkali lavas were emplaced during late Eocene regional subsidence that followed the main magmatic pulse. This sequence of events might record interaction

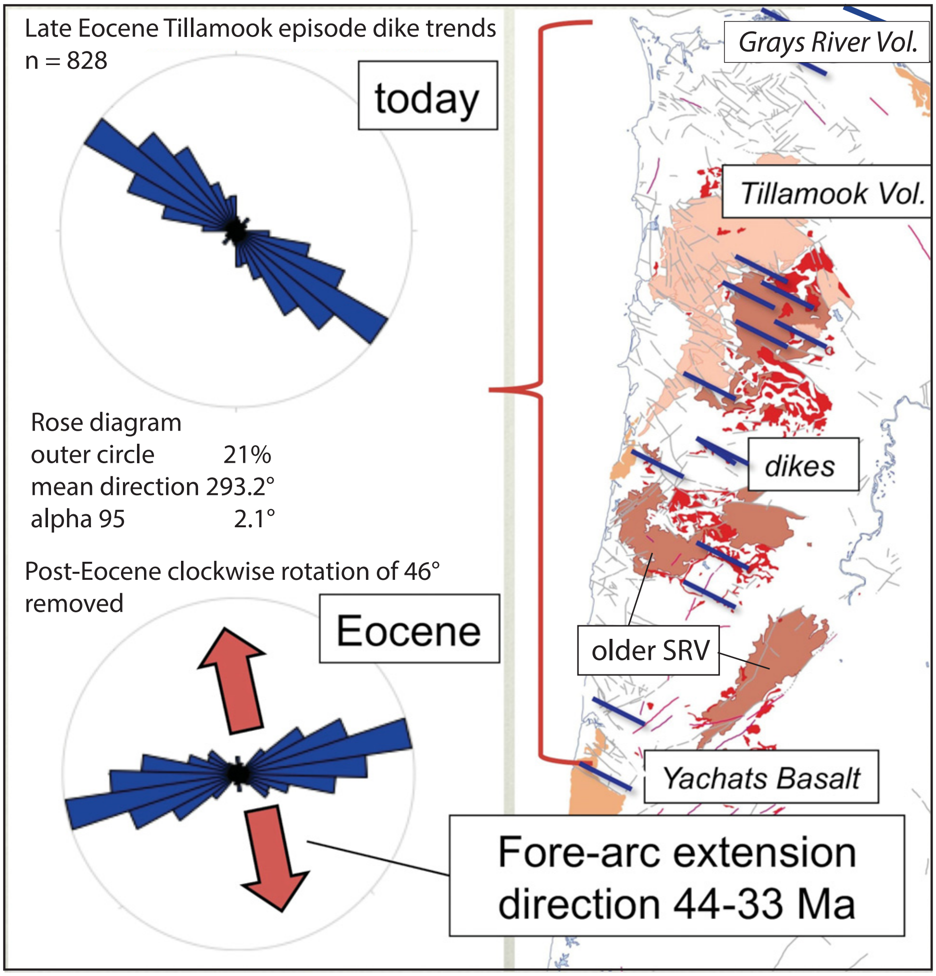

Figure 15. Geologic map showing location and orientation of postaccretion dikes (most are too small to show at scale). Dikes fed pulse of basaltic and alkalic volcanism that initiated ca. 42 Ma and peaked at 41.6 Ma, with decreasing volume to 34 Ma. After back rotation to Eocene orientation, dikes indicate north-northwest–south-southeast–directed extension, parallel to Eocene margin.

with a subducting ridge (Wells et al., 1984; Madsen et al. 2006; McCrory and Wilson, 2013), continued magmatism during subduction zone initiation, or it may reflect interaction of the convergent margin with a hotspot or plume (Duncan, 1982; Chan et al., 2012). We examine these options in the Plate Reconstruction discussion.

ORIGIN OF SILETZIA

Ridge subduction or slab window magmatism may have played an important role in northern Siletzia, where the crust thins to 10 km, sheeted dike swarms crop out beneath the flows on Vancouver Island and in Puget Sound, and the chemistry is compatible with normal type (N) MORB and E-MORB compositions (e.g., Babcock et al., 1992; Fig. 2). Alternatively, the Crescent terrane may represent accreted microplate of normal oceanic crust (McCrory and Wilson, 2013). We suggest that the evidence in Oregon argues for the accretion of an oceanic plateau. (1) The Coast Range basalt is 22–32 km thick, 2–4 times thicker than typical rift crust and similar to an oceanic plateau (Trehu et al., 1994). (2) There are no related feeder dike or sill swarms in the SRV or adjacent continent in Oregon that predate accretion (Wells et al., 2000). (3) There is no early normal faulting. Instead, thrusting during magmatism is followed by later rifting. (4) The SRV basalt sequence is deep submarine to subaerial, not the reverse. (5) The Umpqua sedimentary basin fill progresses from bathyal to subaerial. (6) Umpqua basin sediments lack thermal maturity (Ryu et al., 1996). (7) There is no chemical evidence in lavas or zircons from Eocene coastal silicic rocks of a continental source beneath Siletzia.

Siletzia is a large igneous province (LIP), more than 240,000 km^2 in area, formed in an oceanic environment and composed of thick accumulations of submarine and subaerial tholeiitic and alkalic basalt. The exposed portion was erupted quickly, between 56 and 49 Ma. It is 8–12 times the volume of the Columbia River flood basalt province, based on its forearc extent and thickness inferred from geologic, aeromagnetic, seismic, and well data. Its volume could be much larger, if underplated Siletzia extends to the east beneath the eastern Columbia embayment, as suggested by Schmandt and Humphreys (2011). Many oceanic LIPs can be related to hotspots and/or triple junctions (e.g., Richards et al., 1989, 1991; Nakanishi et al., 1999), and we revisit the idea that Siletzia was produced by an oceanic hotspot close to the continental margin in the early Eocene (Simpson and Cox, 1977; Duncan, 1982; Wells et al., 1984; Murphy et al., 2003; McCrory and Wilson, 2013).

PLATE RECONSTRUCTION

We examine the origin and kinematics of Siletzia and the Yakutat terrane using the plate reconstruction of Seton et al. (2012) as realized in GPlates (www.gplates.org, Gurnis et al., 2012), an open-source interactive plate tectonic visualization software package. In the northeast Pacific basin, the seafloor evidence for the existence of oceanic plates north and east of the Pacific and Farallon plates is largely subducted. Inferences can be made about Kula plate motion from isochrons and fracture zones on the Pacific plate (Engebretson et al., 1985; Lonsdale, 1988; Stock and Molnar, 1988); we can also predict the spreading direction, spreading rate, and strike of the ridge for the vanished Kula-Farallon Ridge from plate tectonic theory (e.g., Engebretson et al., 1985; Stock and Molnar, 1988), although the exact ridge location and possible offsetting transforms are unconstrained.

Several locations and geometries for the Paleogene Kula-Farallon Ridge have been proposed, based largely on onland geologic constraints, and they are used to support a variety of models, including the accretion of Siletzia (Duncan, 1982; Wells et al., 1984; McCrory and Wilson, 2013), the Baja British Columbia hypothesis (Johnston et al., 1996), and slab window models for continental margin magmatism (Breitsprecher et al., 2003; Madsen et al., 2006). In order to explain eastward migration of near-trench magmatism along the southern Alaska margin 60–50 Ma, it was proposed (Haeussler et al., 2003) that an additional plate, the Resurrection plate, occupied the northeast Pacific basin in the Paleogene. Near-trench magmatism would have been produced by subduction of the Kula-Resurrection ridge at the same time as slab window magmatism inboard of the subducting Resurrection-Farallon ridge off the Pacific Northwest.

We accept the simple geometry proposed in the Seton et al. (2012) model as a useful starting point; in the model, a northeast-striking Kula-Farallon Ridge inferred from the northeast Pacific anomalies intersected the northwestern Cordillera for an extended period of time between 60 and 50 Ma (dashed ridge in Fig. 16). We consider the existence of a long-lived Yellowstone hotspot (YHS) to examine how it might have interacted with offshore oceanic plates, probable ridges, and the leading edge of North America. The Seton et al. (2012) model used a hybrid absolute reference frame, based on a moving hotspot model for the past 100 m.y. (see also O'Neill et al., 2005). Although there is no unambiguous geologic track of the YHS prior to ca. 12 Ma (cf. Christiansen et al., 2002; Glen and Ponce, 2002), we reconstruct the position of the YHS as in the O'Neill et al. (2005) reference frame, assuming its existence since at least 60 Ma. Several YHS tracks with respect to North America are shown in Figure 16, and all show northeastward younging toward the present YHS. Differences in the YHS locations at 50 Ma based on Pacific and Atlantic hotspot frames (Müller et al., 1993; Torsvik et al., 2008; Doubrovine et al., 2012; McCrory and Wilson, 2013) in Figure 16 provide some indication of the uncertainties in the Eocene reconstructions. All YHS locations could have provided a source for Siletzia, but note that all arrive early (22 Ma) in the backarc, in the vicinity of the 17 Ma cal-

Figure 16 (*on following page*). Northeast Pacific basin plate reconstruction model of Seton et al. (2012) with Paleogene Yellowstone hotspot (YHS). YHS1 is location with respect to North America in moving hotspot reference frame of O'Neill et al. (2005); YHS2 is in reference frame of Mueller et al. (1993); YHS3 is in reference frame of Doubrovine et al. (2012). (A) 55 Ma: YHS centered on Kula-Farallon Ridge; Siletzia (S) and Yakutat (Y) volcanic ridges inferred to have formed at ridge-centered hotspot since 56 Ma, in V-shaped area of magmatically thickened crust. (B) 55 Ma with Resurrection plate: Possible plate configuration with Resurrection plate. (C) 50 Ma: Accretion of Siletz and Yakutat terranes occurred by 50 Ma, based on stratigraphic onlap relations; sequence of Siletz accretion is shown by small circles. (D) 42 Ma: Following Siletzia accretion, margin encounters YHS, producing northwest-directed extension, dike swarms, and Tillamook magmatic pulse (Tillamook Volcanics) in forearc; Yakutat block moves northwest toward Alaska following Pacific capture of Kula plate. (E) 16 Ma: O'Neill et al. (2005; ON05) and Mueller et al. (1993; M93) hotspot reference frame paths shown by dotted lines; small circles on path show location every 10 m.y. Steens and Columbia River Basalt (CRB) flows in blue; regional Columbia River Basalt–Steens dike swarms in fuchsia (modified from Christiansen et al., 2002); clockwise rotation of Coast Range about a backarc pole continues to move Tillamook Volcanics (TV) and Siletzia northward off YHS track (yellow arrow, ~1°/m.y.). (F) 0 Ma: YHS under Yellowstone (Wyoming); age progression of Snake River Plain calderas (pink) (in Ma); continued clockwise rotation of Coast Range has moved Siletzia off the hotspot track.

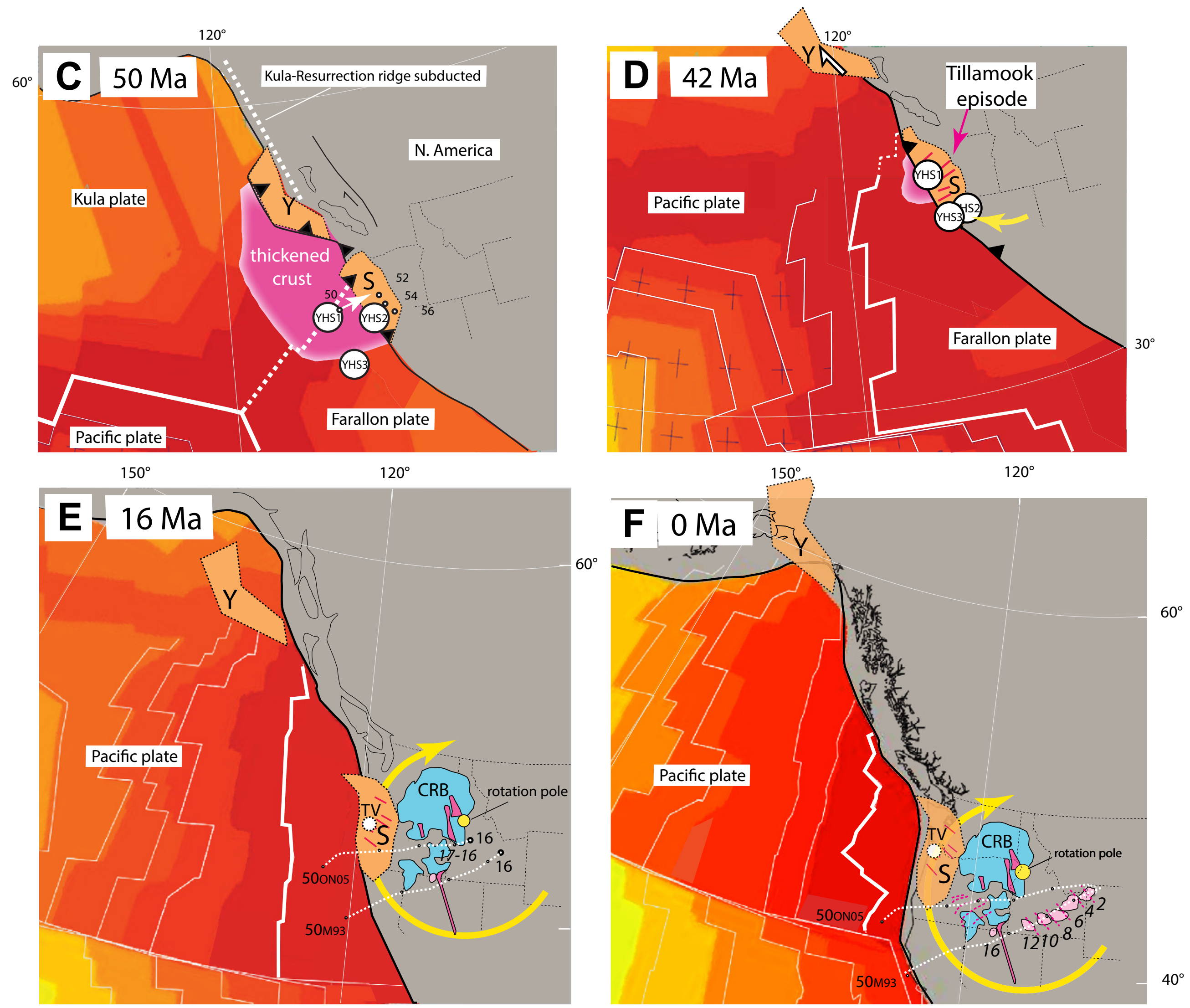
A
55 Ma
crust age, Ma
40
50
30 20 10 0
thickened oceanic crust
Kula plate
N. America
Farallon plate
Pacific plate
B
55 Ma w/ Resurrection plate
Resurrection plate
C
50 Ma
Kula-Resurrection ridge subducted
thickened crust
D
42 Ma
Tillamook episode
E
16 Ma
CRB
rotation pole
TV
50ON05
50M93
F
0 Ma

Figure 16.

deras and flood basalt sources. This may indicate that the YHS has also been moving, likely due to interaction with the subduction margin. Our model is thus permitted by the data, but not definitive.

More complex geometries involving the hypothesized Resurrection plate and its ridges are also possible (Haeussler et al., 2003; McCrory and Wilson, 2013). In the simplest model involving the Resurrection plate, the Resurrection-Farallon ridge has nearly the same orientation as the Kula-Farallon Ridge, and the Resurrection-Kula relative motion is similar to the Kula-Farallon relative motion (Haeussler et al., 2003). In such a model, the origin of Siletzia would be geometrically similar to the Kula-Farallon model prior to ca. 50 Ma, and at 50 Ma, the Kula-Resurrection ridge would have been subducted (Fig. 16).

55 Ma

At 55 Ma the projected Kula-Farallon Ridge passed over or very near the YHS. Two plateaus could have been generated at the YHS, one on the Kula (or Resurrection) and one on the Farallon plate. The geometry may have been similar to the ridges generated at the Galapagos hotspot (O'Connor et al., 2007), where complex interactions between spreading ridge jumps and the hotspot are documented. The plateau on the Farallon plate would have been the progenitor of Siletzia, which initially collided with the continental margin near the present Oregon-California border (42°N; Figs. 2 and 16). A similar model was considered (Wells et al., 1984), but it was thought unlikely that the 13 Ma bilateral age progression reported for Siletzia (by Duncan, 1982) could have been retained, given the long aseismic ridges being subducted, oblique collision, and limited extent of the accreted terrane. Our new ages cut the Siletz age range in half and eliminate the need for accretion of two ridges to form Siletzia. In the present model, 56–50 Ma volcanic centers created at the YHS accreted to southern Oregon at the appropriate time and place, with successive accreted centers becoming younger to the north over a distance of ~300 km, very similar to the observed distribution of ages in Oregon. The collision contributed to the formation of the Columbia embayment, when at least 12°–20° clockwise rotation of the margin occurred. Magmatism continued during collision, allowing deposition of continentally sourced conglomerate interbeds in the pillow basalt. At the northern end of Siletzia, the Kula-Farallon Ridge subducted beneath southern Vancouver Island and the Olympic Peninsula. This produced thinner accreted crust (McCrory and Wilson, 2013), or possibly slab window basalt. Farther north, the YHS produced a basaltic plateau on the Kula (Resurrection) plate, the inferred source of the Eocene Yakutat terrane oceanic basement ca. 55 Ma.

50 Ma

At 50 Ma, the Siletz terrane of Oregon was accreted to the margin of North America and onlapped by coal-bearing strata (Fig. 16; animation in Supplemental File [see footnote 1]). The young, buoyant islands that composed the terrane favored accretion and obduction. During accretion, the subduction zone stepped seaward, and Siletzia became part of North America. Older parts of a greater Siletzia terrane may have been underplated beneath the present backarc region (e.g., Schmandt and Humphreys, 2011). A regional tholeiitic sill complex was emplaced at the top of Siletzia following accretion, possibly a product of upper plate extension following initiation of the new subduction system. Clockwise rotation and northward motion of the forearc began, resulting in prolonged underthrusting of Siletzia beneath Leech River accretionary rocks until 45 Ma. The YHS was just offshore the latitude of Cape Blanco, while the YHS in the Pacific frame is ~500 km offshore.

Farther north, the Yakutat basaltic terrane thrust beneath the Cretaceous Yakutat Formation accretionary complex (Worthington et al., 2012) upon collision with North America ca. 50 Ma. The Yakutat collision point would have been north of Vancouver Island, perhaps near the Queen Charlotte Islands, given 450–900 km of northward displacement of coastal British Columbia terranes since 100 Ma (Wyld et al., 2006; Saleeby and Busby-Spera, 1992) and tens of kilometers of Neogene dextral strike-slip faulting inboard of Queen Charlotte Islands (Rohr and Dietrich, 1992). This is close to the northern option for the location of the Yakutat terrane based on detrital zircon geochronology of onlapping sediments (Perry et al., 2009) and the preferred late Eocene location of Plafker et al. (1994). The deposition of coal-bearing Kultieth sandstones would have occurred on the new terrane shortly after collision, similar to 50–48 Ma deposition of the sandstones of the Umpqua Group and Tyee Formation on Siletzia (Fig. 16). Complete subduction of a Resurrection plate is presumed to have occurred by 50 Ma (dashed line in Fig. 16, 50 Ma panel; Haeussler et al., 2003).

42 Ma

North America, with the accreted Siletzia LIP on its leading edge, ran over the YHS at the latitude of Cape Blanco ca. 42 Ma (Fig. 16; animation in Supplemental File [see footnote 1]). This encounter produced margin-parallel forearc extension and normal faulting, coastal dike swarms from Eugene to Centralia, and the Tillamook-Yachats tholeiitic and alkalic volcanism in the forearc. Trace element and isotopic geochemistry indicate that these lavas had an asthenospheric, plume-like source (Chan et al., 2012; Parker et al., 2010). Diminishing hotspot influence produced lesser 35 Ma volcanism to the north and south of the Tillamook edifice. Magmatism tapered off with scattered alkalic and iron-rich lavas in the Coast Range to 34 Ma. As North America moved westward, the subducting plate, the mantle wedge, and the overlying arc between 34 and 17 Ma masked the YHS hotspot. Rotation of the upper plate about a pole in the backarc begins to move the Tillamook volcanic center northward off the hotspot track ~100 + km between 42 and 17 Ma. Northwestward motion of the Pacific plate 47–43 Ma (Engebretson et al., 1985; Seton et al., 2012) initiated northward transform motion of the Yakutat terrane (Plafker et al., 1994). Between 50 and 42 Ma it may have traveled with coastal British Columbia terranes at 5–9 mm/yr with respect to North America (Wyld et al., 2006), then ca. 42–35 Ma it moved northward at about half the rate of the Pacific plate. The Yakutat terrane is currently moving at nearly the rate of the Pacific plate (47 mm/yr vs. 52 mm/yr; Elliott et al., 2010).

22–16 Ma

Beneath North America, the modeled YHS track in the Indo-Atlantic reference frame (O'Neill et al., 2005) is between the Snake River Plain magmatic progression and the Columbia River Basalt sources at 22 Ma, ~5 m.y. older than the 17 Ma initiation of flood basalt magmatism of the Columbia River Basalt (Camp et al., 2013) and the classic YHS track between 16 and 12 Ma (e.g., Pierce and Morgan, 1992; Christiansen et al., 2002). The YHS tracks in various reference frames bracket the Columbia River Basalt source and the Snake River Plain (Müller et al., 1993; Torsvik et al., 2008; Doubrovine et al., 2012), but the YHS is required to move independently of the Indo-Atlantic reference frame in order to fit the Snake River Plain age progression. We suggest that the YHS track was likely modified by interaction with the subducting plate and southwest rollback of the slab (e.g., Glen and Ponce, 2002; Schmandt and Humphreys, 2011). Melting and storage of magma beneath the slab or melting of the slab may have been facilitated rapid production of the Columbia River flood basalt to form a small LIP (Obrebski et al., 2010). Clockwise rotation of western Oregon continued to move the Tillamook volcanic center northward off YHS track (Wells and McCaffrey, 2013).

0 Ma

The YHS is currently under Yellowstone, Wyoming. Clockwise rotation of the Pacific Northwest continues today, as shown by the contemporary global positioning system (GPS) velocity field (McCaffrey et al., 2007, 2013). Rotation of the Coast Range has moved Siletzia northward, off the hotspot track ~140 km, since 16 Ma (Wells and McCaffrey, 2013). YHS locations relative to North America are shown by dotted lines and circles from GPlates, in 10 m.y. increments (Fig. 16). Since 17 Ma, the calderas of southeast Oregon and the Snake River Plain mark the progression of volcanism toward Yellowstone today (Pierce and Morgan, 1992; Christiansen et al., 2002).

DISCUSSION

Paleogene plate geometries in the northeast Pacific were changeable and probably complex, with spreading-ridge reorganization, ridge subduction, and captured microplates, all fertile ground for basaltic magmatism (cf. Engebretson et al., 1985; Haeussler et al., 2003; Madsen et al., 2006; McCrory and Wilson, 2013). However, the large area and volume of Siletzia, its oceanic composition, short eruption duration, and thick oceanic crust are all characteristic of LIPs (e.g., Bryan and Ernst, 2008). Our age constraints on Siletzia magmatism, geologic constraints on Siletzia composition, volume, and timing of accretion, and kinematic constraints from paleomagnetism, GPS, and modern plate motion models all permit its formation at or near a long-lived YHS, just offshore of North America.

The similarities in age, basalt chemistry, crustal thickness, volume, and early accretionary history between Siletzia and the Yakutat terranes strongly suggest a close relationship between them. Reconstruction of the basaltic basement of the Yakutat terrane to 55–50 Ma brings it southward to the vicinity of the YHS and Kula-Farallon Ridge (or Resurrection-Farallon), adjacent to Siletzia. The Transition fault forming the southern margin of the Yakutat terrane (Fig. 1) reconstructs parallel to the inferred fracture zones along the Kula-Farallon Ridge (Fig. 16).

The formation of the Siletzia and Yakutat LIPs could have been the main event in the magmatic history of the YHS, possibly linked to reorganization of northeast Pacific spreading during Chron 25–22. Rejuvenation of ocean island–type volcanism in the Cascades forearc at 42 Ma during the Tillamook magmatic episode coincides with the expected landfall of a long-lived YHS with the margin of North America, once late Cenozoic northward rotation of the forearc is removed. The 34–17 m.y. gap in volcanism attributable to the YHS we infer is due to the shielding effect of the subducting Farallon plate (e.g., Obrebski et al., 2010). Slab rollback with respect to North America may have pulled the YHS southwest and delayed its appearance, thus explaining the misfit between the modeled tracks and post–17 Ma magmatic history. Initiating YHS activity at 17 Ma in the active backarc (e.g., Christiansen et al., 2002; Hooper et al., 2007; Foulger and Jurdy, 2007; Foulger, 2010; Fouch, 2012) thus reflects emergence of the YHS following rollback and/or melting of the northern Farallon slab, and it is the latest phase of an extended interaction between a convergent margin and a long-lived hotspot. In the long-lived hotspot interpretation, continuation of intraplate magmatism across a subduction boundary requires a magma source moving more slowly than the plates and sourced deeper than the young subducting Farallon plate, which is presumably rolling back as North America advances westward. Recent imaging of the deep structure beneath Yellowstone evidences hot mantle upwelling across the 660 km discontinuity (Schmandt et al., 2012), indicating a source sufficiently deep to survive transit across a convergent margin. In an alternative view, the spatial and temporal sequences of major magmatic events (Siletzia, Tillamook, Columbia River Basalt, Snake River Plain, Yellowstone) along modeled YHS tracks are fortuitous, and all are instead related to a sequence of changing plate boundary conditions, from ridge subduction, oblique marginal rifting, and changing Pacific plate motion. Although plate boundary conditions have played a primary role in the evolution of the Cordillera, we think there is evidence to suggest that a long-lived YHS has contributed to the voluminous Cenozoic magmatism in the Pacific Northwest since at least 56 Ma.

CONCLUSIONS

Siletzia is an oceanic large igneous province, at least 8–12 times the volume of the Columbia River flood basalt province, that accreted to North America between 50.5 and 45 Ma. Detailed geologic mapping of the Siletzia basalts permits correlation of new U-Pb and $^{40}Ar/^{39}Ar$ ages with nannoplankton zones and magnetic polarity, thus showing that Siletzia basalts were rapidly erupted between 56 and 49 Ma, during the Chron 25–22 plate reorganization in the northeast Pacific basin. The crustal thickness of Siletzia varies from 10 to 32 km, and is thickest in the Oregon Coast Range. Thin crust, sheeted dikes, and transitional chemistry may be consistent with ridge or normal subduction in the north, while OIB chemistry, Columbia River Basalt isotopic signatures, and great crustal thickness indicate accretion of an oceanic plateau in Oregon, possibly produced by a long-lived Yellowstone hotspot. Accretion was completed between 50.5 and 49 Ma in Oregon, based on the CP11 age of strata overlying the onlapping continental sediments, and 45 Ma on Vancouver Island, based on cooling ages of the overthrust Leech River schist. During or slightly after accretion (48–45 Ma), a regional tholeiitic MORB sill complex was intruded at the top of Siletzia from Eugene to the Olympic Mountains. We suggest that this event records extension of the overlying plate during initiation of subduction along the new Cascadia subduction zone.

Renewed magmatism, margin-parallel extension, and dike swarm intrusion in the forearc occurred 8 m.y. after accretion. This episode peaked with the rapid eruption of the magnetically reversed Tillamook Volcanics during Chron 19r at 41.6 ± 0.4 Ma, entirely within CP14a. Magmatism continued at a reduced rate until 34 Ma, ending with intrusion of ferrogabbros and nepheline syenites in the forearc. The high volcanic production rates and the high sedimentation rates in the Coast Range have allowed us to correlate most of the Paleocene and Eocene stratigraphic section with the GPTS. This precise age control provides useful constraints on plate models for the origin of Siletzia and its history.

A plate model of the Kula, Farallon, Resurrection, and Pacific plates, along with a long-lived hotspot at the present coordinates of Yellowstone, can provide a nearshore source for Siletzia 56–49 Ma on the Farallon plate and rapid accretion. In the Seton et al. (2012) reconstruction, a, northeast-striking Kula-Farallon Ridge intersects the YHS and is relatively stable, migrating northward along the coast from 40°N to 50°N between 60 and 50 Ma. The similar basaltic Yakutat terrane was derived from the same location, but traveled a more northward course on the Kula (or Resurrection) and Pacific plates.

Although details of the interaction among the ridge, trench, transforms, and moving or fixed YHS cannot truly be known, this model provides for voluminous basaltic magmatism just offshore of the Eocene collision zone. Following accretion of Siletzia, North America overrode the YHS ca. 42 Ma. We suggest that this contributed to the renewed basaltic to alkalic magmatism and margin-parallel extension during the Tillamook magmatic episode in the forearc. Subsequent clockwise rotation, well documented by paleomagnetism and GPS, has moved the Tillamook center northward ~250 km off the likely hotspot track on North America since its formation.

APPENDIX 1. U-PB ANALYTICAL TECHNIQUES

Zircon was separated from rock samples using conventional crushing, grinding, and Wilfley table techniques, followed by final concentration using heavy liquids and magnetic separations. Mineral fractions for analysis were selected based on grain quality, size, magnetic susceptibility, and morphology. Some zircon fractions were air abraded prior to dissolution to minimize the effects of surface-correlated Pb loss, using the technique of Krogh (1982). All grains were washed with warm ultrapure 3N HNO_3 (monazites washed with 1 N HNO_3), rinsed with ultrapure water and subboiled acetone, and weighed (to ±2 mg). Zircons were dissolved in 300 µL PTFE (polytetrafluoroethylene) or PFA (perfluoroalkoxy) microcapsules with ~100 µL of subboiled 29N HF and ~15 µL of subboiled 14N HNO_3 in the presence of a mixed $^{233\text{-}235}$U-^{205}Pb tracer for 40 h at 240 °C. Dissolution took place in stainless-steel Parr bombs with 250 mL Teflon PTFE liners. Sample solutions were then dried to salts at ~125 °C and rebombed in ultrapure ~200 µL 3.1N HCl for 12 h at 210 °C. Pb and U separation for both zircon and monazite employed ion-exchange column techniques similar to those described by Parrish et al. (1987). Pb and U were eluted sequentially into the same beaker followed by the addition of ~10 µL of 0.6N ultrapure phosphoric acid. Each sample was loaded onto a single zone refined Re filament using a phosphoric acid–silica gel emitter ($SiCl_4$). Isotopic ratios were measured using a modified single collector VG-54R thermal ionization mass spectrometer equipped with an analogue Daly photomultiplier. Both U and Pb were run at 1300–1450 °C, in peak-switching mode on the Daly detector. U fractionation was determined directly on individual runs using the $^{233\text{-}235}$U tracer, and Pb isotopic ratios were corrected for fractionation of 0.37%/amu, based on replicate analyses of the NBS-981 Pb standard and the values recommended by Thirlwall (2000). U analytical blanks were <1 pg and Pb generally <3 pg. Common Pb isotopic compositions are derived from the model of Stacey and Kramer (1975). Data reduction employed the Excel-based program of Schmitz and Schoene (2007). Standard concordia diagrams were constructed and regression intercepts and weighted averages calculated with Isoplot (Ludwig, 2003). Unless otherwise noted all errors are quoted at the 2σ or 95% level of confidence. Isotopic dates are calculated with the decay constants l_{238} = 1.55125E-10 and l_{235} = 9.8485E-10 (Jaffe et al., 1971).

ACKNOWLEDGMENTS

We thank Joe Vance for generously sharing his zircon samples, Karen Wheeler for help in extracting maps from detailed geographic information system databases, Chris DuRoss for help constructing the Roseburg cross section, and Zdenek Venera for discussion and help with the fault kinematics program. We also thank Kris McElwee for access to unpublished K/Ar and Ar/Ar ages, Joe Colgan for help with U-Pb ages, and Mark Turner and Simon Williams for assistance with GPlates. Parke Snavely, Jr. and David Engebretson provided early encouragement for this project. We thank Gene Humphreys for helpful discussion and Sean Gulick, Pat McCrory, Terry Pavlis, and Derek Thorkelson for very thoughtful reviews.

REFERENCES CITED

Allmendinger, R.W., Cardozo, N.C., and Fisher, D., 2012, Structural geology algorithms: Vectors and tensors: Cambridge, UK, Cambridge University Press, 289 p.

Babcock, R.S., and Hirsch, D.M., 2006, Geochemistry and petrology of a thick sequence of Crescent Basalt in the Dosewallips River Valley, Olympic Peninsula, Washington State: Geological Society of America Abstracts with Programs, v. 38, no. 5, p. 95.

Babcock, R.S., Burmester, R.F., Engebretson, D.C., Warnock, A., and Clark, K.P., 1992, A rifted margin origin for the Crescent Basalts and related rocks in the northern Coast Range volcanic province, Washington and British Columbia: Journal of Geophysical Research, v. 97, p. 6799–6821, doi:10.1029/91JB02926.

Baldwin, E.M., 1974, Eocene stratigraphy of southwestern Oregon: Oregon Department of Geology and Mineral Industries Bulletin 83, 40 p.

Barnes, M.A., and Barnes, C.G., 1992, Petrology of late Eocene lavas at Cascade Head, Oregon Coast Range: Journal of Volcanology and Geothermal Research, v. 52, p. 157–170, doi:10.1016/0377-0273(92)90138-4.

Beck, M.E., 1984, Has the Washington-Oregon Coast Range moved northward?: Geology, v. 12, p. 737–740, doi:10.1130/0091-7613(1984)12<737:HTWCRM>2.0.CO;2.

Beck, M.E., and Plumley, P.W., 1980, Paleomagnetism of intrusive rocks in the Coast Range of Oregon: Microplate rotations in middle Tertiary time: Geology, v. 8, p. 573–577, doi:10.1130/0091-7613(1980)8<573:POIRIT>2.0.CO;2.

Blake, M.C., Jr., Engebretson, D.C., Jayko, A.S., and Jones, D.L., 1985, Tectono-stratigraphic terranes in southwest Oregon, *in* Howell, D.G., et al., eds., Tectonostratigraphic terranes of the circum-Pacific region: Circum-Pacific Council for Energy and Mineral Resources Earth Science Series, v. 1, p. 147–157.

Blakely, R.J., Sherrod, B.L., Hughes, J.F., Anderson, M.L., Wells, R.E., and Weaver, C.S., 2009, Saddle Mountain fault deformation zone, Olympic Peninsula, Washington—Western boundary of the Seattle uplift: Geosphere, v. 5, p. 105–125, doi:10.1130/GES00196.1.

Boyden, J.A., Müller, R.D., Gurnis, M., Torsvik, T.H., Clark, J.A., and Turner, M., Ivey-Law, Hamish, Watson, R.J., and Cannon, J. S., 2011, Next-generation plate-tectonic reconstructions using GPlates: Geoinformatics: Cyberinfrastructure for the Solid Earth Sciences, p. 95–114.

Breitsprecher, K., Thorkelson, D.J., Groome, W.G., and Dostal, J., 2003, Geochemical confirmation of the Kula-Farallon slab window beneath the Pacific Northwest in Eocene time: Geology, v. 31, p. 351–354, doi:10.1130/0091-7613(2003)031<0351:GCOTKF>2.0.CO;2.

Brocher, T.M., Parsons, T., Blakely, R.J., Christiensen, N.I., Fisher, M.A., and Wells, R.E., and the SHIPS Working Group, 2001, Upper crustal structure in Puget Lowland, Washington: Results from the 1998 seismic hazards investigation in Puget Sound: Journal of Geophysical Research, v. 106, p. 13,541–13,564, doi:10.1029/2001JB000154.

Bryan, S.E., and Ernst, R.E., 2008, Revised definition of large igneous provinces (LIPs): Earth-Science Reviews, v. 86, no. 1, p. 175–202, doi:10.1016/j.earscirev.2007.08.008.

Bruns, T.R., 1983, Model for the origin of the Yakutat block, an accreting terrane in the northern Gulf of Alaska: Geology, v. 11, no. 12, p. 718–721, doi:10.1130/0091-7613(1983)11<718:MFTOOT>2.0.CO;2.

Bukry, D., 1971, Cenozoic calcareous nannofossils from the Pacific Ocean: San Diego Society of Natural History Transactions, v. 16, p. 303–327.

Bukry, D., 1973, Low-latitude coccolith biostratigraphic zonation, *in* Edgar, N.T., et al., Initial reports of the Deep Sea Drilling Project, Volume 15: Washington, D.C., U.S. Government Printing Office, p. 685–703, doi:10.2973/dsdp.proc.15.116.1973.

Bukry, D., and Snavely, P.D., Jr., 1988, Coccolith zonation for Paleogene strata in the Oregon Coast Range, *in* Filewicz, M.V., and Squires, R.L., eds., Paleogene stratigraphy, West Coast of North America: Pacific Section, Society of Economic Paleontologists and Mineralogists West Coast Paleogene Symposium, v. 58, p. 251–263.

Camp, V.E., Ross, M.E., Duncan, R.A., Jarboe, N.A., Coe, R.S., Hanan, B.B., and Johnson, J.A., 2013, The Steens basalt: Earliest lavas of the Columbia River basalt group, *in* Reidel, S.P., et al., eds., The Columbia River flood basalt province: Geological Society of America Special Paper 497, p. 87–116, doi:10.1130/2013.2497(04).

Chan, C.F., Tepper, J.H., and Nelson, B.K., 2012, Petrology of the Grays River volcanics, southwest Washington: Plume-influenced slab window magmatism in the Cascadia forearc: Geological Society of America Bulletin, v. 124, p. 1324–1338, doi:10.1130/B30576.1.

Christeson, G.L., Gulick, S.P.S., van Avendonk, H.J.A., Worthington, L.L., Reece, R.S., and Pavlis, T.L., 2010, The Yakutat terrane: Dramatic change in crustal thickness across the Transition fault, Alaska: Geology, v. 38, p. 895–898, doi:10.1130/G31170.1.

Christiansen, R.L., Foulger, G.R., and Evans, J.R., 2002, Upper mantle origin of the Yellowstone hotspot: Geological Society of America Bulletin, v. 114, p. 1245–1256, doi:10.1130/0016-7606(2002)114<1245:UMOOTY>2.0.CO;2.

Clowes, R.M., Brandon, M.T., Green, A.G., Yorath, C.J., Brown, A.S., Kanasewich, E.R., and Spencer, C., 1987, LITHOPROBE-southern Vancouver Island: Cenozoic subduction complex imaged by deep seismic reflections: Canadian Journal of Earth Sciences, v. 24, p. 31–51, doi:10.1139/e87-004.

Colgan, J.P., and Henry, C.D., 2009, Rapid middle Miocene collapse of the Mesozoic orogenic plateau in north-central Nevada: International Geology Review, v. 51, p. 920–961, doi:10.1080/00206810903056731.

Courtillot, V., Davaillie, A., Besse, J., and Stock, J., 2003, Three distinct types of hotspots in the Earth's mantle: Earth and Planetary Science Letters, v. 205, p. 295–308, doi:10.1016/S0012-821X(02)01048-8.

Davis, A.S., and Plafker, G., 1986, Eocene basalts from the Yakutat terrane: Evidence for the origin of an accreting terrane in southern Alaska: Geology, v. 14, p. 963–966, doi:10.1130/0091-7613(1986)14<963:EBFTYT>2.0.CO;2.

Davis, A.S., Snavely, P.D., Jr., Gray, L.B., and Minasian, D.L., 1995, Petrology of Late Eocene Lavas Erupted in the Forearc of Central Oregon: U.S. Geological Survey Open-File Report 95-40, 58 p.

Dickinson, W.R., 2004, Evolution of the North American cordillera: Annual Review of Earth and Planetary Sciences, v. 32, p. 13–45, doi:10.1146/annurev.earth.32.101802.120257.

Diller, J.S., 1898, Roseburg folio: Geologic Atlas of the United States, Folio 49: Washington, D.C., U.S. Geological Survey, 4 p., scale 1:125,000.

Doubrovine, P.V., Steinberger, B., and Torsvik, T.H., 2012, Absolute plate motions in a reference frame defined by moving hot spots in the Pacific, Atlantic, and Indian Oceans: Journal of Geophysical Research, v. 117, B09101, doi:10.1029/2011JB009072.

Dumitru, T.A., Ernst, W.G., Wright, J.E., Wooden, J.L., Wells, R.E., Farmer, L.P., Kent, A.J.R., and Graham, S.A., 2013, Eocene extension in Idaho generated massive sediment floods into Franciscan trench and into the Tyee, Great Valley, and Green River basins: Geology, v. 41, p. 187–190, doi:10.1130/G33746.1

Duncan, R.A., 1982, A captured island chain in the Coast Range of Oregon and Washington: Journal of Geophysical Research, v. 87, p. 10827–10837, doi:10.1029/JB087iB13p10827.

DuRoss, C.B., Blakely, R.J., and Wells, R.E., 2002, Geologic cross sections through the Roseburg 30′ × 60′ quadrangle, Oregon: New constraints from potential field modeling: Geological Society of America Abstracts with Programs, v. 34, no. 5, p. 32.

Eberhart-Phillips, D., Christensen, D.H., Brocher, T.M., Hansen, R., Ruppert, N.A., Haeussler, P.J., and Abers, G.A., 2006, Imaging the transition from Aleutian subduction to Yakutat collision in central Alaska, with local earthquakes and active source data: Journal of Geophysical Research, v. 111, B11303, doi:10.1029/2005JB004240.

Elliott, J.L., Larsen, C.F., Freymueller, J.T., and Motyka, R.J., 2010, Tectonic block motion and glacial isostatic adjustment in southeast Alaska and adjacent

Canada constrained by GPS measurements: Journal of Geophysical Research, v. 115, B09407, doi:10.1029/2009JB007139.

Engebretson, D.C., Cox, A., and Gordon, R.G., 1985, Relative motions between oceanic and continental plates in the Pacific Basin: Geological Society of America Special Paper 206, 60 p., doi:10.1130/SPE206.

Ewing, T.E., 1980, Paleogene tectonic evolution of the Pacific Northwest: Journal of Geology, v. 88, p. 619–638, doi:10.1086/628551.

Fouch, M.J., 2012, The Yellowstone hotspot: Plume or not?: Geology, v. 40, p. 479–480, doi:10.1130/focus052012.1.

Foulger, G.R., 2010, Plates vs. plumes: A geological controversy: Oxford, UK, Wiley-Blackwell, 360 p.

Foulger, G.R., and Jurdy, D.M., eds., 2007, Plates, plumes, and planetary processes: Geological Society of America Special Paper 430, 974 p., doi:10.1130/978-0-8137-2430-0(2007)430[ix:P]2.0.CO;2.

Gao, H., Humphreys, E.D., Yao, H., and van der Hilst, R.D., 2011, Crust and lithosphere structure of the northwestern US with ambient noise tomography: Terrane accretion and Cascade arc development: Earth and Planetary Science Letters, v. 304, p. 202–211, doi:10.1016/j.epsl.2011.01.033.

Glen, J.M.G., and Ponce, D.A., 2002, Large-scale fractures related to inception of the Yellowstone hotspot: Geology, v. 30, p. 647–650, doi:10.1130/0091-7613(2002)030<0647:LSFRTI>2.0.CO;2.

Gradstein, F.M., Ogg, J.G., Schmitz, M., and Ogg, G., 2012, The geologic time scale 2012: Amsterdam, Elsevier, 1176 p.

Grommé, C.S., Beck, M.E., Jr., Wells, R.E., and Engebretson, D.C., 1986, Paleomagnetism of the Tertiary Clarno Formation and its significance for the tectonic history of the Pacific Northwest: Journal of Geophysical Research, v. 91, p. 14,089–14,103, doi:10.1029/JB091iB14p14089.

Groome, W.G., Thorkelson, D.J., Friedman, R.M., Mortensen, J.K., Massey, N.W.D., Marshall, D.D., and Layer, P.W., 2003, Magmatic and tectonic history of the Leech River Complex, Vancouver Island, British Columbia: Evidence for ridge-trench intersection and accretion of the Crescent terrane, *in* Sisson, V.B., et al., eds., Geology of a transpressional orogen developed during ridge-trench interaction along the North Pacific margin: Geological Society of America Special Paper 371, p. 327–353, doi:10.1130/0-8137-2371-X.327.

Gulick, S., Reece, R.S., Christeson, G.L., Van Avendonk, H., Worthington, L.L., and Pavlis, T.L., 2013, Seismic images of the Transition fault and the unstable Yakutat–Pacific–North American triple junction: Geology, v. 41, p. 571–574, doi:10.1130/G33900.1.

Gurnis, M., Hall, C., and Lavier, L., 2004, Evolving force balance during incipient subduction: Geochemistry Geophysics Geosystems, v. 5, Q07001, doi:10.1029/2003GC000681.

Gurnis, M., Turner, M., Zahirovic, S., DiCaprio, L., Spasojevic, S., Müller, R.D., Boyden, J., Seton, M., Manea, V.C., and Bower, D.J., 2012, Plate tectonic reconstructions with continuously closing plates: Computers & Geosciences, v. 38, no. 1, p. 35–42, doi:10.1016/j.cageo.2011.04.014.

Haeussler, P.J., and Clark, K.P., 2000, Geologic map of the Wildcat Lake 7.5′ quadrangle, Kitsap and Mason Counties, Washington: U.S. Geological Survey Open-File Report 00-356, scale 1:24,000.

Haeussler, P.J., Bradley, D.C., Wells, R.E., and Miller, M.L., 2003, Life and death of the Resurrection plate: Evidence for an additional plate in the northeastern Pacific in Paleocene–Eocene time: Geological Society of America Bulletin, v. 115, p. 867–880, doi:10.1130/0016-7606(2003)115<0867:LADOTR>2.0.CO;2.

Hamilton, W., and Myers, W.B., 1966, Cenozoic tectonics of the western United States: Reviews of Geophysics, v. 4, p. 509–549, doi:10.1029/RG004i004p00509.

Heller, P.L., and Ryberg, P.T., 1983, Sedimentary record of subduction to forearc transition in the rotated Eocene basin of western Oregon: Geology, v. 11, p. 380–383, doi:10.1130/0091-7613(1983)11<380:SROSTF>2.0.CO;2.

Hirsch, D.M., and Babcock, R.S., 2009, Spatially heterogeneous burial and high-P/T metamorphism in the Crescent Formation, Olympic Peninsula, Washington: American Mineralogist, v. 94, p. 1103–1110, doi:10.2138/am.2009.3187.

Hooper, P.R., Camp, V.E., Reidel, S.P., and Ross, M.E., 2007, The origin of the Columbia River flood basalt province: Plume versus nonplume models, *in* Foulger, G.R., and Jurdy, D.M., eds., Plates, plumes, and planetary processes: Geological Society of America Special Paper 430, p. 635–668, doi:10.1130/2007.2430(30).

Irving, E., 1964, Paleomagnetism and its application to geological and geophysical problems: New York: Wiley, 399 p.

Irving, E., 1979, Paleopoles and paleolatitudes of North America and speculatiions about displaced terrains: Canadian Journal of Earth Sciences, v. 16, p. 669–694, doi:10.1139/e79-065.

Johnston, S.T., and Acton, S., 2003, The Eocene southern Vancouver Island orocline—A response to seamount accretion and the cause of fold-and-thrust belt and extensional basin formation: Tectonophysics, v. 365, p. 165–183, doi:10.1016/S0040-1951(03)00021-0.

Kleibacker, D.W., 2001, Sequence stratigraphy and lithofacies of the middle Eocene upper McIntosh and Cowlitz Formations, geology of the Grays River volcanics, Castle Rock–Germany Creek area, southwest Washington [M.S. thesis]: Corvallis, Oregon, Oregon State University, 215 p.

Krogh, T.E., 1982, Improved accuracy of U-Pb zircon ages by the creation of more concordant systems using an air abrasion technique: Geochimica et Cosmochimica Acta, v. 46, p. 637–649, doi:10.1016/0016-7037(82)90165-X.

Lipman, P., 1995, Declining growth of Mauna Loa during the last 100,000 years: Rates of lava accumulation vs. gravitational subsidence, *in* Rhodes, J.M., and Lockwood, J.P., eds., Mauna Loa revealed: Structure, composition, history, and hazards: American Geophysical Union Geophysical Monograph 92, p. 45–80 doi:10.1029/GM092p0045.

Lipman, P.W., and Calvert, A.T., 2013, Modeling volcano growth on the Island of Hawaii: Deep-water perspectives: Geosphere, v. 9, p. 1348–1383, doi:10.1130/GES00935.1.

Lonsdale, P., 1988, Paleogene history of the Kula plate: Offshore evidence and onshore implications: Geological Society of America Bulletin, v. 100, no. 5, p. 733–754, doi:10.1130/0016-7606(1988)100<0733:PHOTKP>2.3.CO;2.

Ludwig, K.R., 2003, User's manual for Isoplot 3.00: A geochronological toolkit for Microsoft Excel: Berkeley Geochronology Center Special Publication 4, 74 p.

Madsen, J.K., Thorkelson, D.J., Friedman, R.M., and Marshall, D.D., 2006, Cenozoic to recent plate configurations in the Pacific Basin: Ridge subduction and slab window magmatism in western North America: Geosphere, v. 2, p. 11–34, doi:10.1130/GES00020.1.

Magill, J.R., and Cox, A.V., 1980, Tectonic rotation of the Oregon Western Cascades: Oregon Department of Geology and Mineral Industries Special Paper 10, 67 pp.

Magill, J., Cox, A., and Duncan, R.A., 1981, Tillamook volcanic series: Further evidence for tectonic rotation of the Oregon Coast Range: Journal of Geophysical Research, v. 86, no. B4, p. 2953–2970, doi:10.1029/JB086iB04p02953.

Massey, N.W.D., 1986, Metchosin Igneous Complex, southern Vancouver Island: Ophiolite stratigraphy developed in an emergent island setting: Geology, v. 14, p. 602–605, doi:10.1130/0091-7613(1986)14<602:MICSVI>2.0.CO;2.

McCaffrey, R., Qamar, A.I., King, R.W., Wells, R.E., Ning, Z., Williams, C.A., Stevens, C.W., Vollick J.J., and Zwick, P.C. 2007, Fault locking, block rotation, and crustal deformation in the Pacific Northwest: Geophysical Journal International, v. 169, p. 1315–1340, doi:10.1111/j.1365-246X.2007.03371.x.

McCaffrey, R., King, R.W., Payne, S.J., and Lancaster, M., 2013, Active tectonics of northwestern US inferred from GPS-derived surface velocities: Journal of Geophysical Research, v. 118, p. 709–723, doi:10.1029/2012JB009473.

McCrory, P.A., and Wilson, D.S., 2013, A kinematic model for the formation of the Siletz-Crescent forearc terrane by capture of coherent fragments of the Farallon and Resurrection plates: Tectonics, v. 32, p. 718–736, doi:10.1029/2013TC.

Molenaar, C.M., 1985, Depositional relations of Umpqua and Tyee formations (Eocene), southwestern Oregon: American Association of Petroleum Geologists Bulletin, v. 69, p. 1217–1229.

Moothart, S.R., 1993, Geology of the middle and upper Eocene Mcintosh Formation and adjacent volcanic and sedimentary rock units, Willapa Hills, Pacific County, southwest Washington [M.S. thesis]: Corvallis, Oregon State University, 265 p.

Müller, R.D., Royer, J.Y., and Lawver, L.A., 1993, Revised plate motions relative to the hotspots from combined Atlantic and Indian Ocean hotspot tracks: Geology, v. 21, p. 275–278, doi:10.1130/0091-7613(1993)021<0275:RPMRTT>2.3.CO;2.

Murphy, J.B., Hynes, A.J., Johnston, S.T., and Keppie, J.D., 2003, Reconstructing the ancestral Yellowstone plume from accreted seamounts and its relationship to flat-slab subduction: Tectonophysics, v. 365, p. 185–194, doi:10.1016/S0040-1951(03)00022-2.

Nakanishi, M., Sager, W.W., and Klaus, A., 1999, Magnetic lineations within Shatsky Rise, northwest Pacific Ocean: Implications for hot spot-triple junction interaction and oceanic plateau formation: Journal of Geophysical Research, v. 104, B4, p. 7539–7556, doi:10.1029/1999JB900002.

Niem, A.R., and Niem, W.A., 1985, Oil and gas investigations of the Astoria Basin, Clatsop and northernmost Tillamook Counties, northwest Oregon: Oregon Department of Geology and Mineral Industries Oil and Gas Investigation 14, scale 1:100,000.

Obrebski, M., Allen, R.M., Xue, M., and Hung, S., 2010, Slab-plume interaction beneath the Pacific Northwest: Geophysical Research Letters, v. 37, L14305, doi:10.1029/2010GL043489.

O'Connor, J.M., Stoffers, P., Wijbrans, J.R., and Worthington, T.W., 2007, Migration of widespread long-lived volcanism across the Galápagos Volcanic Province: Evidence for a broad hotspot melting anomaly?: Earth and Planetary Science Letters, v. 263, p. 339–354, doi:10.1016/j.epsl.2007.09.007.

Okada, H., and Bukry, J.D., 1980, Supplementary modification and introduction of code numbers to the low-latitude coccolith biostratigraphic zonation (Bukry, 1973; 1975): Marine Micropaleontology, v. 5, p. 321–325, doi:10.1016/0377-8398(80)90016-X.

O'Neill, C., Müller, D., and Steinberger, B., 2005, On the uncertainties in hotspot reconstructions and the significance of moving hotspot reference frames: Geochemistry Geophysics Geosystems, v. 6, no. 4, Q04003, doi:10.1029/2004GC000784.

Oxford, J., 2006, Early Oligocene intrusions in the Central Coast Range of Oregon: Petrography, geochemistry, geochronology, and implications for the Tertiary magmatic evolution of the Cascadia forearc [M.S. thesis]: Corvallis, Oregon State University, 236 p.

Parker, D.F., Hodges, F.N., Perry, A., Mitchener, M.E., Barnes, M.A., and Ren, M., 2010, Geochemistry and petrology of late Eocene Cascade Head and Yachats Basalt and alkalic intrusions of the central Oregon Coast Range, USA: Journal of Volcanology and Geothermal Research, v. 198, p. 311–324, doi:10.1016/j.jvolgeores.2010.09.016.

Parrish, R., Roddick, J.C., Loveridge, W.D., and Sullivan, R.W., 1987, Uranium-lead analytical techniques at the geochronology laboratory, *in* Radiogenic age and isotopic studies, Report 1: Geological Survey of Canada Paper 87-2, p. 3–7.

Parsons, T., Trehu, A.M., Luetgert, J.H., Miller, K., Kilbride, F., Wells, R.E., Fisher, M.A., Flueh, E., ten Brink, U.S., and Christiansen, N.I., 1998, A new view into the Cascadia subduction zone and volcanic arc: Implications for earthquake hazards along the Washington margin: Geology, v. 26, p. 199–202, doi:10.1130/0091-7613(1998)026<0199:ANVITC>2.3.CO;2.

Parsons, T., Wells, R.E., Fisher, M.A., Flueh, E., and ten Brink, U.S., 1999, Three-dimensional velocity structure of Siletzia and other accreted terranes in the Cascadia fore arc of Washington: Journal of Geophysical Research, v. 104, p. 18,015–18,039, doi:10.1029/1999JB900106.

Payne, C.W., 1998, Lithofacies, stratigraphy, and geology of the middle Eocene type Cowlitz Formation and associated volcanic and sedimentary units, eastern Willapa Hills, southwest Washington [M.S. thesis]: Corvallis, Oregon, Oregon State University, 235 p.

Perry, S.E., Garver, J.I., and Ridgway, K.D., 2009, Transport of the Yakutat terrane, southern Alaska: Evidence from sediment petrology and detrital zircon fission-track and U-Pb double dating: Journal of Geology, v. 117, p. 156–173, doi:10.1086/596302.

Phillips, W.M., Walsh, T.J., and Hagen, R.A., 1989, Eocene transition from oceanic to arc volcanism, southwest Washington: U.S. Geological Survey Open-File Report 89–178, p. 199–256.

Pierce, K.L., and Morgan, L.A., 1992, The track of the Yellowstone hot spot: Volcanism, faulting, and uplift, Link, P. K., Kuntz, M. A., and Platt, L. B., eds., Regional geology of eastern Idaho and western Wyoming: Geological Society of America Memoir 179, p. 1-53.

Plafker, G., 1987, Regional geology and petroleum potential of the northern Gulf of Alaska continental margin, *in* Scholl, D.W., et al., eds., Geology and resource potential of the continental margin of western North America and adjacent ocean basins—Beaufort Sea to Baja California: Circum-Pacific Council for Energy and Mineral Resources Earth Science Series, v. 6, p. 229–268.

Plafker, G., Moore, J.C., and Winkler, G.R., 1994, Geology of the southern Alaska margin, *in* Plafker, G., and Berg, H.C., eds., The Geology of Alaska: Boulder, Colorado, Geological Society America, Geology of North America, v. G-1, pp. 389–450.

Pyle, D.G., 1988, Geochemical evolution of the Roseburg Formation basaltic rocks, southern Oregon Coast Range [M.S. thesis]: Corvallis, Oregon State University, 137 p.

Pyle, D., Duncan, R., Wells, R.E., Graham, D.W., Harrison, B., and Hanan, B., 2009, Siletzia: An oceanic large igneous province in the Pacific Northwest: Geological Society of America Abstracts with Programs, v. 41, no. 7, p. 369.

Rarey, P.J., 1985, Geology of the Hamlet-North Fork of the Nehalem River area, southern Clatsop and northernmost Tillamook counties, northwest Oregon [M.S. thesis]: Corvallis, Oregon State University, 457 p.

Reidel, S.P., 2013, The Columbia River flood basalt province: Stratigraphy, areal extent, volume, and physical volcanology, *in* Reidel, S.P., et al., eds., The Columbia River flood basalt province: Geological Society of America Special Paper 497, p. 1–44, doi:10.1130/2013.2497(01).

Richards, M.A., Jones, D.L., Duncan, R.A., and DePaolo, D.J., 1991, A mantle plume initiation model for the Wrangellia flood basalt and other oceanic plateaus: Science, v. 254, p. 263–267, doi:10.1126/science.254.5029.263.

Richards, M.A., Duncan, R.A., and Courtillot, V.E., 1989, Flood basalts and hot-spot tracks: Plume heads and tails: Science, v. 246, p. 103–107, doi:10.1126/science.246.4926.103.

Rohr, K.M.M., and Dietrich, J.R., 1992, Strike-slip tectonics and development of the Tertiary Queen Charlotte Basin, offshore western Canada: Evidence from seismic reflection data: Basin Research, v. 4, p. 1–20, doi:10.1111/j.1365-2117.1992.tb00039.x.

Ryu, In-Chang, Niem, A.R., and Niem, W.A., 1996, Oil and gas potential of the southern Tyee Basin, southern Oregon Coast Range: Oregon Department of Geology and Mineral Industries Oil and Gas Investigations 19, p. 109–124.

Saleeby, J.B., and Busby-Spera, C., 1992, Early Mesozoic tectonic evolution of the western U.S. Cordillera, *in* Burchfiel, B.C., Lipman, P.W., and Zoback, M.L., eds., The Cordilleran orogen: Conterminous U.S.: Boulder, Colorado, Geological Society of America, Geology of North America, v. G-3, p. 107–168.

Santra, M., Steel, R.J., Olariu, C., and Sweet, M.L., 2013, Stages of sedimentary prism development on a convergent margin—Eocene Tyee forearc basin, Coast Range, Oregon, USA: Global and Planetary Change, v. 103, p. 207–231, doi:10.1016/j.gloplacha.2012.11.006.

Schmandt, B., and Humphreys, E., 2011, Seismically imaged relict slab from the 55 Ma Siletzia accretion to the northwest United States: Geology, v. 39, p. 175–178, doi:10.1130/G31558.1.

Schmandt, B., Dueker, K., Humphreys, E., and Hansen, S., 2012, Hot mantle upwelling across the 660 beneath Yellowstone: Earth and Planetary Science Letters, v. 331, p. 224–236, doi:10.1016/j.epsl.2012.03.025.

Schmitz, M.D., and Schoene, B., 2007, Derivation of isotope ratios, errors, and error correlations for U-Pb geochronology using ^{205}Pb-^{235}U-(^{233}U)-spiked isotope dilution thermal ionization mass spectrometric data: Geochemistry Geophysics Geosystems, v. 8, Q08006, doi:10.1029/2006GC001492.

Scholl, D. W., and von Huene, R., 2010, Subduction zone recycling processes and the rock record of crustal suture zones: Canadian Journal of Earth Sciences, v. 47, no. 5, p. 633–654.

Seton, M., and 10 others, 2012, Global continental and ocean basin reconstructions since 200 Ma: Earth-Science Reviews, v. 113, p. 212–270, doi:10.1016/j.earscirev.2012.03.002.

Simpson, R.W., 1977, Paleomagnetic evidence for tectonic rotation of the Oregon Coast Range: Thesis (Ph.D.), Stanford University, Stanford California, 156 p.

Simpson, R.W., and Cox, A., 1977, Paleomagnetic evidence for tectonic rotation of the Oregon Coast Range: Geology, v. 5, p. 585–589, doi:10.1130/0091-7613(1977)5<585:PEFTRO>2.0.CO;2.

Snavely, P.D., Jr., 1987, Tertiary geologic framework, neotectonics, and petroleum potential of the Oregon-Washington continental margin, *in* Scholl, et al., eds., Geology and resource potential of the continental margin of western North America and adjacent ocean basins–Beaufort Sea to Baja California: Circum-Pacific Council for Energy and Mineral Resources Earth Science Series, v. 6, p. 305–335.

Snavely, P.D., Jr., and Baldwin, E.M., 1948, Siletz River Volcanic series, northwestern Oregon: American Association of Petroleum Geologists Bulletin, v. 32, p. 805–812.

Snavely, P.D., MacLeod, N.S., and Wagner, H.C., 1968, Tholeiitic and alkali basalts of the Eocene Siletz River Volcanics, Oregon Coast Range: American Journal of Science, v. 266, p. 454–481, doi:10.2475/ajs.266.6.454.

Snavely, P.D., Jr., and MacLeod, N.S., 1974, Yachats Basalt—An upper Eocene differentiated volcanic sequence in the Oregon Coast Range: U.S. Geological Survey Journal of Research, v. 2, p. 395–403.

Snavely, P.D., Jr., MacLeod, N.S., Wagner, H.C., and Rau, W.W., 1976a, Geologic map of the Cape Foulweather and Euchre Mountain quadrangles, Lincoln County, Oregon: U.S. Geological Survey Miscellaneous Investigations Map I-868, scale 1:62,500.

Snavely, P.D., Jr., MacLeod, N.S., Wagner, H.C., and Rau, W.W., 1976b, Geologic map of the Yaquina and Toledo quadrangles, Lincoln County, Oregon: U.S. Geological Survey Miscellaneous Investigations Map 1-867, scale 1:62,500.

Snavely, P.D., Jr., MacLeod, N.S., Wagner, H.C., and Rau, W.W., 1976c, Geologic map of the Waldport and Tidewater quadrangles, Lincoln, Lane, and Benton Counties, Oregon: U.S. Geological Survey Miscellaneous Investigation Series Map 1-866, scale 1:62,500.

Snavely, P.D., Jr., Bukry, D., and Wells, R.E., 1993a, Coccolith-bearing late middle Eocene Kerogen Shale, Tillamook Highlands, northwest Oregon Coast Range: U.S. Geological Survey Open-File Report 93-623, 13 p.

Snavely, P.D., Jr., MacLeod, N.S., and Niem, A.R., 1993b, Geologic map of Cape Flattery, Clallam Bay, Ozette Lake, and Lake Pleasant quadrangles, northwestern Olympic Peninsula, Washington: U.S. Geological Survey Miscellaneous Investigations Series Map I-1946, scale 1:48,000.

Snavely, P.D., Niem, Alan, Wong, F.L., MacLeod, N.S., Calhoun, T.K., Minasian, D.L., and Niem, Wendy, 1996, Geologic map of the Cascade Head area, northwestern Oregon Coast Range (Neskowin, Nestucca Bay, Hebo, and Dolph 7.5 minute quadrangles): U.S. Geological Survey Open-File Report OF-96-534, scale 1:24,000.

Squires, R.L., Goedert, J.L., and Kaler, K.L., 1992, Paleontology and stratigraphy of Eocene rocks at Pulali point, Jefferson County, eastern Olympic Peninsula, Washington: Washington Division of Geology and Earth Resources Report of Investigations 31, 27 p.

Stacey, J.S., and Kramer, J.D., 1975, Approximation of terrestrial lead isotope evolution by a two-stage model: Earth and Planetary Science Letters, v. 26, p. 207–221, doi:10.1016/0012-821X(75)90088-6.

Stock, J.M., and Molnar, P., 1988, Uncertainties and implications of the Late Cretaceous and Tertiary position of North America relative to the Farallon, Kula, and Pacific plates: Tectonics, v. 7, p. 1339–1384, doi:10.1029/TC007i006p01339.

Tabor, R.W., and Cady, W.M., 1978, Geologic map of the Olympic Peninsula, Washington: U.S. Geological Survey Miscellaneous Investigations Series Map I-994, scale 1:125,000.

Tabor, R.W., Haugerud, R.A., Haeussler, P.J., and Clark, K.P., 2011, Lidar-revised geologic map of the Wildcat Lake 7.5′ Quadrangle, Kitsap and Mason Counties, Washington: U.S. Geological Survey Scientific Investigations Map 3187, scale 1:24,000, 12 p.

Thirlwall, M.F., 2000, Inter-laboratory and other errors in Pb isotope analyses investigated using a ^{207}Pb-^{204}Pb double spike: Chemical Geology, v. 163, p. 299–322, doi:10.1016/S0009-2541(99)00135-7.

Thorkelson, D.J., 1996, Subduction of diverging plates and the principles of slab window formation: Tectonophysics, v. 255, p. 47–63, doi:10.1016/0040-1951(95)00106-9.

Torsvik, T.H., Müller, R.D., Van der Voo, R., Steinberger, B., and Gaina, C., 2008, Global plate motion frames: Toward a unified model: Reviews of Geophysics, v. 46, no. 3, RG3004, doi:10.1029/2007RG000227.

Trehu, A.M., Asudeh, I., Brocher, T.M., Luetgert, J.H., Mooney, W.D., Nabelek, J.L., and Nakamura, Y., 1994, Crustal architecture of the Cascadia forearc: Science, v. 266, p. 237–243, doi:10.1126/science.266.5183.237.

Walker, G.W., and Duncan, R.A., 1988, Geologic map of the Salem 1° by 2° quadrangle, Oregon: U.S. Geological Survey Miscellaneous Investigations Map I-1893, scale 1:250,000.

Wells, R.E., 1981, Geologic map of the eastern Willapa Hills, Cowlitz, Lewis, Pacific, and Wahkiakum Counties, Washington: U.S. Geological Survey Open-File Report 81-674, scale 1:62,500.

Wells, R.E., 1989a, Geologic map of the Cape Disappointment–Naselle River area, Pacific and Wahkiakum Counties, Washington: U.S. Geological Survey Miscellaneous Investigations Map I-1832, scale 1:62,500.

Wells, R.E., 1989b, Mechanisms of Cenozoic tectonic rotation, Pacific Northwest convergent margin, U.S.A., *in* Kiessel, C., and Laj, C., eds., Paleomagnetic rotations and continental deformation: NATO Advanced Study Institute Volume C254: Netherlands, Kluwer Publishers, p. 313–325.

Wells, R.E., and Coe, R.S., 1985, Paleomagnetism and geology of Eocene volcanic rocks of southwest Washington, implications for mechanisms of tectonic rotation: Journal of Geophysical Research, v. 90, p. 1925–1947, doi:10.1029/JB090iB02p01925.

Wells, R.E., and McCaffrey, R., 2013, Steady rotation of the Cascade Arc: Geology, v. 41, p. 1027–1030, doi:10.1130/G34514.1.

Wells, R.E., and Sawlan, M.G., 2014, Preliminary geologic map of the eastern Willapa Hills, Cowlitz, Lewis, Pacific, and Wahkiakum Counties, Washington: U.S. Geological Survey Open-File Report 2014-1063, scale 1:50,000.

Wells, R.E., Engebretson, D.C., Snavely, P.D., and Coe, R.S., 1984, Cenozoic plate motions and the volcano-tectonic evolution of western Oregon and Washington: Tectonics, v. 3, p. 275–294, doi:10.1029/TC003i002p00275.

Wells, R.E., Snavely, P.D., Jr., Macleod, N.S., Kelly, M.M., and Parker, M.J., Fenton, J., and Felger, T., 1995, Geologic map of the Tillamook Highlands, northwest Oregon Coast Range—A digital database: U. S. Geological Survey Open-File Report 95-670, http://pubs.usgs.gov/of/1995/of95-670/.

Wells, R.E., Weaver, C.S., and Blakely, R.J., 1998, Forearc migration in Cascadia and its neotectonic significance: Geology, v. 26, p. 759–762, doi:10.1130/0091-7613(1998)026<0759:FAMICA>2.3.CO;2.

Wells, R.E., Jayko, A., Niem, A.R., Black, G., Wiley, T., Baldwin, E., Molenaar, K.M., Wheeler, K., Givler, R., and DuRoss, C., 2000, Geologic map and database of the Roseburg, Oregon 30′ × 60′ Quadrangle, Douglas and Coos Counties, Oregon: U.S. Geological Survey Open-File Report OF00-376, 55 p., scale 1:100,000.

Wolfe, E.W., and McKee, E.H., 1968, Geology of the Grays River Quadrangle, Wahkiakum and Pacific Counties, Washington: Washington Division of Mines and Geology Geologic Map GM-4, scale 1:62,500.

Worthington, L.L., Gulick, S.P., and Pavlis, T.L., 2010, Coupled stratigraphic and structural evolution of a glaciated orogenic wedge, offshore St. Elias orogen, Alaska: Tectonics, v. 29, TC6013, doi:10.1029/2010TC002723.

Worthington, L.L., Van Avendonk, H.J.A., Gulick, S.P.S., Christeson, G.L., and Pavlis, T.L., 2012, Crustal structure of the Yakutat terrane and the evolution of subduction and collision in southern Alaska: Journal of Geophysical Research, v. 117, B01102, doi:10.1029/2011JB008493.

Wyld, S.J., Umhoefer, P.J., and Wright, J.E., 2006, Reconstructing northern Cordilleran terranes along known Cretaceous and Cenozoic strike-slip faults: Implications for the Baja British Columbia hypothesis and other models, *in* Haggart, J.W., et al., eds., Paleogeography of the North American Cordillera: Evidence for and against large-scale displacements: Geological Association of Canada Special Paper 46, p. 277–298.

Yorath, C.J., Brown, A.S., and Massey, N.W.D., 1999, Lithoprobe, southern Vancouver Island, British Columbia: Geology: Geological Survey of Canada Bulletin 498, 145 p.